p. 116

THE EFFECT OF ELASTIC BOUNDARY CONDITIONS ON THE DYNAMIC RESPONSE OF RECTANGULAR PLATES

by

Terry K. Brewer
B.S. May 1980, Salisbury State College
B.S. May 1985, Old Dominion University

A Thesis Submitted to the Faculty of
Old Dominion University in Partial Fulfillment of the
Requirements for the Degree of

MASTER OF ENGINEERING

ENGINEERING MECHANICS

OLD DOMINION UNIVERSITY
May, 1988

Approved by:

Chuh Mei (Director)

John S. Mixson

Jean W. Hou

ABSTRACT

THE EFFECT OF ELASTIC BOUNDARY CONDITIONS ON THE DYNAMIC RESPONSE OF RECTANGULAR PLATES

Terry K. Brewer
Old Dominion University
Director: Dr. Chuh Mei

Natural frequencies and forced steady-state harmonic response for the vibration of uniform rectangular plates with edges elastically restrained against rotation and transverse translation are addressed. A single mode Rayleigh-Ritz solution is derived using functions that describe the normal modes of vibration of a beam whose ends are elastically restrained. The finite element solution is obtained for comparison. MACSYMA symbolic manipulation system is implemented as an aid to the mathematical rigor of the Ritz approach and NASTRAN finite element code is used to model the mechanical system. Comparisons are made to published results and the solutions of this study are found to give lower frequencies for some values of boundary restraint. Steady-state harmonic amplitudes of displacement and acceleration are found to agree favorably for the two solutions. Low predictions of steady-state strain from NASTRAN result in some cases when compared to the Ritz values. Finally, a subjective assessment is made about the merit of using MACSYMA and NASTRAN.

TABLE OF CONTENTS

ACKNOWLEDGEMENT

This thesis was partially supported by NAS1-17993-22 at NASA-Langley Research Center in Hampton, Virginia.

LIST OF TABLES

TABLE PAGE

LIST OF FIGURES

FIGURE PAGE

CHAPTER 1

Introduction

Research studies of plate vibrations under various loadings, plate geometries and panel types have received wide attention since the 1950's due mainly to the applications of these studies to the fatigue failures of aircraft structures. Until recently, design of the structures has been largely based on empirical nomographs (1-3) but as new materials (including composites and high temperature materials) gain wider applications to aerospace vehicles, the development of design charts is economically limited. Currently, these new materials are generally reserved for "low risk" applications. As a result, there is a need to produce and improve analytical procedures to accurately predict panel response.

Since the predicted and measured bending strain of conventional aluminum rectangular panels can typically differ by a factor of two or more, studies have been made to assess the accuracy of classical linear small deflection plate theory. Roussos, Heitman and Rucker (4) encountered an even greater discrepancy in 1986 as predicted strain values were approximately three times higher than those measured. Although these results may be "safe" from a design standpoint,

the optimization of design is sacrificed. This large bias error prompted the investigation of the effect of boundary conditions on the response of rectangular plates (5). In particular, the interest was focused on edges that are restrained by both rotational and translational boundary springs.

Previous experimentation was conducted on four panel types including isotropic (aluminum), orthotropic and two anisotropic plates. The mounting of the boundaries was done utilizing a rubber gasket scheme on both sides of the panels with double gasket thickness on the load source side. The load source delivered an acoustic excitation at levels of 80 to 120 dB. These low levels of normally incident plane waves were used to apply a uniform spatial load at constant temperature. The horn speaker produced low frequency (60 to 2000 Hz.) noise as the sound field was mapped and the pressure spectrum was analyzed. The panels were measured for fundamental resonance frequencies and critical damping ratio. However, the edge restraint values were not experimentally determined but were considered uniform on each edge by virtue of the rubber gaskets.

The analytical models employed for comparison of measured acceleration and strain response displayed only rotational boundary restraints with edges rigidly supported in the transverse direction. The accompanying analysis was performed by a Rayleigh-Ritz frequency response formulation and a supplemental response calculation was done on the isotropic panel by a finite element method. The boundary values used were

determined by requiring good fundamental frequency prediction and close agreement to ratios of x and y strain measurements. The measured accelerations closely matched those predicted. Unfortunately, the measured and predicted strain response differed by the aforementioned bias for all panels tested. In a search for causes, the finite element model was extended to include the elastic transverse boundary conditions. In the comparison to measurements, the relaxation of transverse edge motion accompanying rotational edge elasticity could not account for such a large bias. Fault for the discrepancy was tentatively placed on the strain gages chosen for testing.

To date, most of tne analysis of elastically restrained plates has been done using the Rayleigh-Ritz energy formulation although the Galerkin method and numerical techniques have been utilized (6,7). In the Rayleigh-Ritz approach, the maximum strain energy is equated to the maximum kinetic energy of the plate and by assuming a finite linear series of displacement functions that satisfy the geometric boundary conditions , the natural frequencies, mode shapes and consequently, the overall response may then be solved for. Much of this work has been presented using polynomials as the assumed displacement functions since the resulting calculations and computations are made simpler. This approach has been shown to be adequate to obtain natural frequencies and mode shapes for lower modes of vibration (8). It is also advantageous when the study includes nonrectangular plates, nonuniform thickness and plates with geometric discontinuity

because of the simplicity of the assumed polynomial functional relation (9,10).

Since the accuracy of the Rayleigh-Ritz approximation depends, to a large extent, on the "closeness" of the assumed displacement functions to the true mode shape, many analysts feel the use of characteristic modes of beam vibration in the method is a better choice. The underlying assumption is that in a given coordinate direction, a slim strip of the plate will approximate the behavior of a vibrating beam. The plate is then modeled as a continuous collection of beams in two directions. This choice of functions has been demonstrated to give greater accuracy especially for the natural frequencies of higher modes and in the case of mixed classical boundary conditions (11). Classical boundary conditions are traditionally regarded as clamped, simply supported and free edges and can be mixed among the four edges to yield 21 combinations.

It should be noted that the Rayleigh-Ritz method and other techniques used to solve problems of rectangular plate vibrations are merely approximations, in general. Exact solutions to the differential equation of transverse vibrations exist only for the cases of paired simply supported parallel edges. Of the 21 possible combinations of classical boundary conditions, these exact solutions comprise only six cases. By excluding the free edge cases and imposing mounting constraints, the number of classical boundary exact solutions drops to three. These three are the cases of a plate with all boundaries simply supported, three edges simply supported with

one end clamped and two opposite edges simply supported with clamped conditions on the remaining two boundaries. Since, in reality, there are no perfectly clamped or simply supported edges, it is reasonable to restrain the boundaries with continuous rotational and/or translational springs. The classical edge conditions become special cases with appropriately assigned spring constants. For example, the simply supported edge is achieved by imposing a rotational spring value of zero and a transverse foundation spring value of infinity. With these considerations included, practical mounting of a rectangular plate is more realistically modeled.

In 1983, Warburton and Edney (12) presented the Rayleigh-Ritz method utilizing suitable combinations of modal functions of beams with classical boundary conditions to study elastically restrained plates. As an example, the natural frequencies of a panel with parallel edges restrained against rotation are intermediate between those of plate with opposite edges simply supported and those with opposing edges clamped. The assumed mode shape is a summation of simply supported-simply supported, simply supported-clamped, clamped-simply supported and clamped-clamped characteristic beam functions in the appropriate coordinate direction. In this way, combinations of the limiting values of the rotational restraint parameters on each edge are included in the analysis and the classical functions can be weighted to give the intermediate values. By incorporating the free edge and sliding edge conditions of beams into the procedure, translational boundary restraints may be included

also. This method proved to give good accuracy when compared to the results of previous authors and was shown to be relatively easy to use since the integrals of beam functions that result in the Rayleigh-Ritz approach and the characteristic frequency parameters for classical boundary conditions are well documented. The underlying purpose of Warburton and Edney was to give designers rapid and inexpensive estimates of natural frequencies of practical plates with applications to many modes of vibrations, aspect ratios and edge restraint parameters.

One of the methods used for comparison by Warburton and Edney was given by Carmichael in 1959 (13). Carmichael also used the Rayleigh-Ritz procedure. The analysis treated plates with rotational edge restraint only whereby all boundaries were considered rigidly restrained against translation. Accordingly, Carmichael assumed displacement functions that represent the normal modes of vibration of a beam whose ends are elastically restrained against rotation and rigid in the transverse direction. This approach necessitated the development of integrals of these elastically supported beam functions and he also generated a closed form approximate frequency expression from a single term solution. This approximate frequency was shown to be quite accurate as compared to the frequency from a multi-term solution.

Other studies of elastically restrained plate vibrations are usually compared to those mentioned when relative merit is sought. Analysts have given quick methods for natural frequency calculations and tables of values for the use of a

given approach. However, there is a loss of generality associated with some derivations as the authors restrict themselves to a specific problem with simplified assumptions. For example, only recently has attention been given to the case of edges possessing two distinct types of boundary springs. Prior to this, a presentation might treat problems exhibiting only symmetric rotational boundary springs and/or square plate geometries. In order to further these methods to a larger class of problems, it becomes necessary to "rework" the entire problem. Thus, the application of an approach can be long and arduous.

Another difficulty associated with the implementation of an analytic technique is the brevity of published treatise. Often, the answers sought and presented are limited to the extraction of natural frequencies and mode shapes related to free vibration of the plate so that examples of numerical results of displacements, accelerations and strains are not implied or referred to. As a result, the engineer using the technique to predict forced response must finish the problem. This is not always simple if functional expressions for numerical calculations are desired. The mathematical manipulation required to obtain a completed solution can be algebraically difficult and seemingly impossible. Usually, an assessment is made to decide if the extra analysis is practical in both time and expense of the work. If the labor is pursued, it becomes necessary to evaluate the results by comparison to real problems.

The comparisons made by many authors is a third pertinent topic. Quite often, the evaluation of an operational algorithm is limited to a comparison with a procedure that is similar in derivation. Intuitively, the two approaches yield similar results. The studies are not usually compared to dissimilar formulations of the same problem. Since prediction of structural behavior is the ultimate goal of these studies, comparisons are required to different solutions and to measured response from experimentation.

In order to adequately address the topics of elastically restrained rectangular plate vibrations, the present treatise again utilizes the Rayleigh-Ritz method. However, the assumed displacement functions are given by the normal modes of beams whose ends are unsymmetrically restrained against rotation and translation. This is an extension of Carmichael's approach and necessitates the derivation of the beam solution and the generation of the resulting beam integrals. In this way, unlimited combinations of distinct rotational and linear spring parameters can be included. Variation of aspect ratio can also be considered.

Because of the complexities in the mathematical rigor associated with this type of solution, a symbolic manipulation program is used as an aid in the analytic derivation. The program chosen is MACSYMA since it is very comprehensive in it's mathematical capabilities and it is well documented. The differentiation and integration required are effectively executed as program commands. The evaluation

of boundary conditions and simultaneous equation algorithms are available to the user. It is possible to generate an analytic solution and to program numerical procedures of problems in rectangular plate vibrations completely on the computer. This has great potential when compared to "hand-cranking" an analytical derivation.

The comparisons of solutions includes results from previous authors where applicable as well as the comparison to a finite element formulation. The well known finite element code, NASTRAN, is utilized. The choice of NASTRAN was also based on availability and comprehensive capabilities. These comparisons allow the assessments of accuracy of solutions and numerical results. This evaluation also gives an estimation to the relative contribution value of available engineering and mathematical computer software.

More specifically,the purpose of this thesis is to study the effect of elastic boundary conditions on the dynamic displacement and strain frequency response of rectangular uniform plates. The loading is assumed to have a deterministic frequency spectrum that can be represented by a finite series of harmonic inputs. The loading amplitude is assumed uniform over the plate surface. The direction is to normal incidence. Parameter studies are made for plates at several aspect ratios for predicted natural frequencies versus elastic restraint values. Studies include trend analyses for steady-state displacement and strain response.

Two methods are used to conduct these studies. They are the Rayleigh-Ritz method and the finite element method. Comparisons are made to previous accepted results to verify the two methods as solution techniques. The Rayleigh-Ritz approach is aided by MACSYMA symbolic manipulation program. NASTRAN finite element code is utilized. A subjective assessment is made of the relative contribution of MACSYMA and NASTRAN as computational aids.

The contributions of this thesis include the use of beam functions representative of the elastic boundary conditions in the Rayleigh-Ritz approach and the extension of the method to predict measurable response.

Classical linear small deflection plate theory is assumed throughout the analysis.

CHAPTER 2

Rayleigh-Ritz Energy Formulation

Theoretical Basis

In 1877, Lord Rayleigh used the principle of conservation of energy to obtain an expression for the fundamental natural frequency of an undamped linear structure under free vibration (14). He argued that as the structure vibrates harmonically at it's natural frequency, the potential energy given when vibration is at maximum amplitudes is exchanged for the energy of a purely kinetic state when amplitudes are zero. The maximum potential energy of bending, $V_{max,b}$, of a plate is determined by the strain energy stored in the plate. It should be noted, however, that $V_{max,b}$ from plate bending is not necessarily equal to the total maximum potential energy, V_{max}, since additional terms in V_{max} may result from other energy storage sources such as boundary springs, for example. For the case of the aforementioned classical boundary conditions, $V_{max,b} = V_{max}$.

The maximum kinetic energy, T_{max}, is taken while the plate vibrates at it's natural frequency and the fundamental frequency can be calculated by minimizing the following equation,

$$T_{max} - V_{max} = \text{stationary value} \qquad (1)$$

Ideally, the expression given in equation (1) is identically zero. However, this only occurs when the true mode displacement function is used to determine V_{max} and T_{max}. Since exact solutions to rectangular plate vibrations are not known, in general, equation (1) is minimized with respect to the assumed displacement functions. This reduces the resulting nonzero error to a minimal stationary value. If the assumed displacement function satisfies all the boundary conditions, the calculated natural frequency obtained has been shown to be an upper bound. That is, the true structural frequency is lower than that calculated. The reason for this is that using an assumed mode in the procedure is equivalent to an additional constraint which raises the potential energy and calculated frequency. The Rayleigh formulation frequency approaches the exact from above as the greater accuracy criteria dictates.

For example, the bending strain of a uniform rectangular plate can be shown to be given by,*

$$V_{max} = \frac{D}{2}\int_0^a\int_0^b (W_{,xx}^2 + W_{,yy}^2 + 2\mu W_{,xx} W_{,yy} + 2(1-\mu)W_{,xy}^2)\,dydx \qquad (2)$$

where for now it is assumed $V_{max,b} = V_{max}$, and where the comma denotes partial differentiation with respect to the variables following the comma.

---

* Notation convention is given in Appendix A.

The maximum kinetic energy is given by,

$$T_{max} = \rho \frac{h}{2} \omega^2 \int_0^a \int_0^b W^2(x,y) \, dydx \qquad (3)$$

where $w = W(x,y)e^{i\omega t}$ is the assumed transverse displacement function over the spatial domain vibrating at the fundamental frequency, ω . The i denotes $\sqrt{(-1)}$.

For the ideal case (stationary value=0), substituting equations (2) and (3) into (1) and solving yields,

$$\omega^2 = \frac{V_{max}}{\rho \frac{h}{2} \int_0^a \int_0^b W(x,y)^2 \, dydx} \qquad (4)$$

Equation (4) is called the Rayleigh Quotient.

In order to obtain frequencies beyond the fundamental, Ritz developed an extension of the Rayleigh formulation. The estimated mode function is assumed to be a finite linear series with arbitrary constant coefficients, C_r . The minimization of equation (1) then becomes,

$$\frac{\partial}{\partial C_r} (V - T) = 0 \quad , \quad (r=1,2,3,...n) \qquad (5)$$

Equation (5) results in n homogeneous equations that can be solved for n-1 constants in terms of the remaining constant. When the finite series is truncated at r=1, equation (5) reduces exactly to equation (4) for the determination of fundamental frequency while C_1 is arbitrary. The remaining

constant represents an amplitude and for free vibration of the plate, it is dependent on the initial conditions. For the case of steady state harmonic forced response, the amplitude constant is dependent on the amplitude and frequency of the forcing function. When n>1, equation (5) can be written in matrix form and effectively becomes an eigenvalue problem with mass and stiffness contributions arising from the kinetic and potential energies, respectively. The natural frequencies are obtained from the condition that the determinant of the system of equations is zero.

Considerations of Boundary Conditions

Ideally, all boundary conditions are satisfied by the chosen displacement functions. However, previous methodology (14) has shown that sufficient accuracy of frequency prediction can be achieved by satisfying only the geometric boundary conditions (ie. displacement and slope) while neglecting the dynamic or natural boundary conditions (ie. shear and moment). The accuracy is dependent on the true type of edge conditions for a case under study. For example, the clamped edge has only geometric boundary conditions, $W(o,y)=0$ and $W_{,x}(o,y)=0$, and the Rayleigh-Ritz method gives quite good frequency results with appropriately chosen functions. When the edges are restrained elastically, the boundary conditions can be considered natural only. The choice of functions that satisfy geometric conditions can result in loss of accuracy.

For the plate shown in figure (1), the rotational boundary conditions are given by,

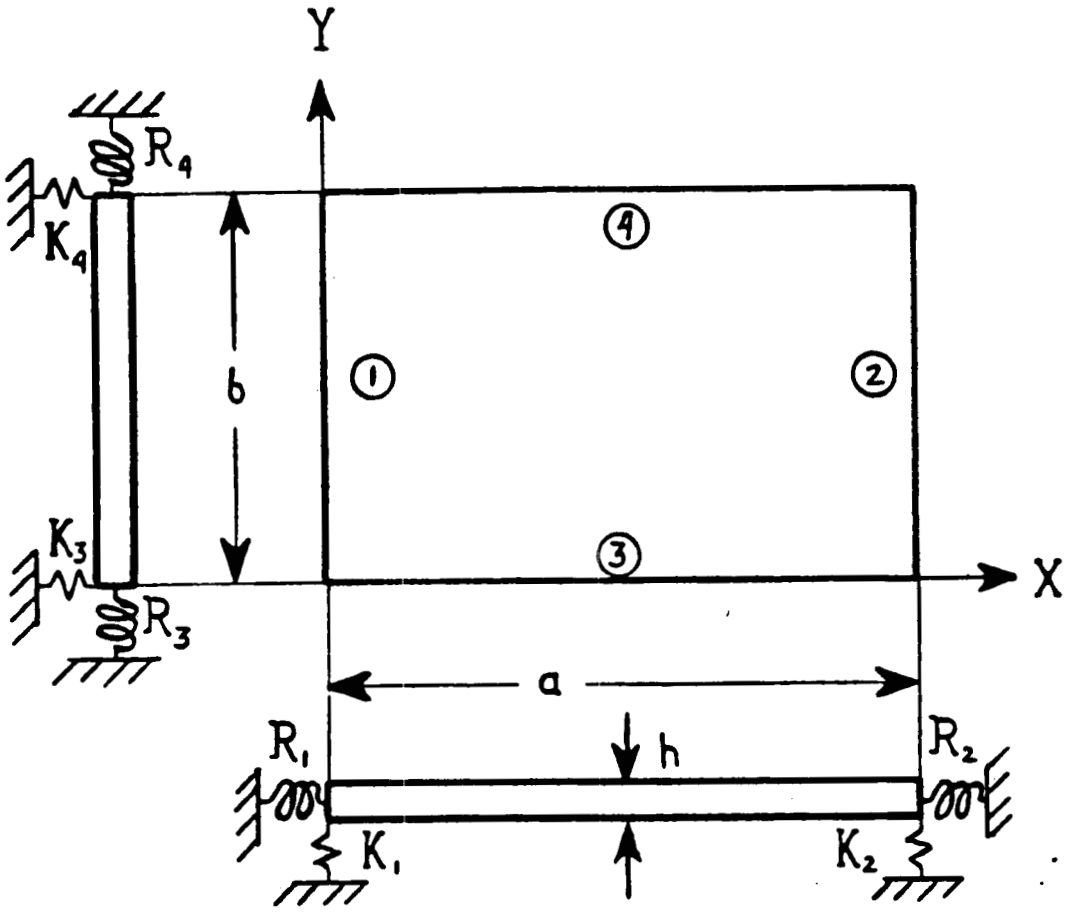

Figure (1). Mechanical System Under Study

$$R_1 W_{,x}(o,y) = D(W_{,xx}(o,y) + \mu W_{,yy}(o,y)) \tag{6A}$$

$$R_2 W_{,x}(a,y) = -D(W_{,xx}(a,y) + \mu W_{,yy}(a,y)) \tag{6B}$$

$$R_3 W_{,y}(x,o) = D(W_{,yy}(x,o) + \mu W_{,xx}(x,o)) \tag{6C}$$

$$R_4 W_{,y}(x,b) = -D(W_{,yy}(x,b) + \mu W_{,xx}(x,b)) \tag{6D}$$

where R_i is the bending moment (per unit length) for unit rotation on the i th edge, (i=1,2,3,4).

The translational boundary conditions of the plate are given by,

$$K_1 W(o,y) = -D(W_{,xxx}(o,y) + (2- \mu)W_{,xyy}(o,y)) \quad (7A)$$

$$K_2 W(a,y) = D(W_{,xxx}(a,y) + (2- \mu)W_{,xyy}(a,y)) \quad (7B)$$

$$K_3 W(x,o) = -D(W_{,yyy}(x,o) + (2- \mu)W_{,yxx}(x,o)) \quad (7C)$$

$$K_4 W(x,b) = D(W_{,yyy}(x,b) + (2- \mu)W_{,yxx}(x,b)) \quad (7D)$$

where K_i is the transverse edge reaction (per unit length) for unit displacement on the i th edge, (i=1,2,3,4).

Equations (6)-(7) are simplified if in addition to uniform elastic stiffness, twisting on each edge is not restrained. That is, the moments about an axis parallel to a given edge and the vertical shear on that edge are directly restrained by the boundary springs. The boundary conditions become,

$$R_1 W_{,x}(o,y) = D(W_{,xx}(o,y)) \quad (6A')$$

$$R_2 W_{,x}(a,y) = -D(W_{,xx}(a,y)) \quad (6B')$$

$$R_3 W_{,y}(x,o) = D(W_{,yy}(x,o)) \quad (6C')$$

$$R_4 W_{,y}(x,b) = -D(W_{,yy}(x,b)) \quad (6D')$$

$$K_1 W(o,y) = -D(W_{,xxx}(o,y)) \quad (7A')$$

$$K_2 W(a,y) = D(W_{,xxx}(a,y)) \quad (7B')$$

$$K_3\, W(x,o) = -D(W_{,yyy}(x,o)) \tag{7C'}$$

$$K_4\, W(x,b) = D(W_{,yyy}(x,b)) \tag{7D'}$$

The boundary conditions given by equations (6')-(7') are assumed in this analysis and the beam functions used are chosen so as to satisfy these conditions. All in-plane motion at the boundaries is prohibited since the assumption of linear small deflection theory renders these motions negligible. That is, for small amplitude plate vibrations, the transverse bending and the in-plane membrane oscillations are uncoupled and independent. With this in mind, translational motion at the edges is meant as transverse motion only.

Choice of Assumed Displacement Functions

The general form of the finite series to represent displacement in the Rayleigh-Ritz method for harmonic steady state rectangular plate vibrations is given by,

$$w(x,y,t) = W(x,y)\, e^{i\omega t} \tag{8}$$

where $w(x,y,t)$ is assumed to be separable in x,y and t. The spatial variation, $W(x,y)$, is,

$$W(x,y) = \sum_{m=1}^{p}\sum_{n=1}^{q} A_{mn}\, X_m(x)\, Y_n(y) \tag{9}$$

such that $X_m(x)$ and $Y_n(y)$ are chosen to satisfy the boundary conditions while m and n are modal identification

indices. The beam functions selected are given by,

$$X_m(x) = B_m \sinh\left(\frac{\alpha_m x}{a}\right) + C_m \sin\left(\frac{\alpha_m x}{a}\right) + D_m \cosh\left(\frac{\alpha_m x}{a}\right) + \cos\left(\frac{\alpha_m x}{a}\right) \tag{10}$$

$$Y_n(y) = E_n \sinh\left(\frac{\beta_n y}{b}\right) + F_n \sin\left(\frac{\beta_n y}{b}\right) + G_n \cosh\left(\frac{\beta_n y}{b}\right) + \cos\left(\frac{\beta_n y}{b}\right) \tag{11}$$

where B, C, D, α, E, F, G and β are constants obtained from the application of equations (6′)-(7′). The results are given in Appendix B.

By noting the similarity of x to y in the equations (10)-(11) and also in equations (6′)-(7′), the respective constants are of like form. That is, once B, C, D and α are determined from equations (6A′), (6B′), (7A′),(7B′) and (10), E, F, G and β result by substituting y for x, E for B, F for C, G for D, β for α, n for m, R_3 for R_1, R_4 for R_2, K_3 for K_1, K_4 for K_2 and b for a.

Derivation of Solution

The differential equation that governs the motion of a uniform plate subject to an external loading is given by,

$$D\nabla^4 w + \rho h \ddot{w} + c \dot{w} = p \tag{12}$$

where ρh is mass per unit area (ρ = mass density) and c is the damping coefficient.

The pressure, $p = p(x,y,t)$, is assumed to be harmonic and uniformly distributed which results in an harmonic

displacement, $w = w(x,y,t)$. Using complex notation,

$$p = p(x,y,t) = P(x,y)\, e^{i\omega t} = P\, e^{i\omega t} \tag{13}$$

and,

$$w = w(x,y,t) = W(x,y)\, e^{i\omega t} \tag{14}$$

where $P(x,y)$ and $W(x,y)$ are the spatial amplitudes of pressure and displacement, respectively. For a uniform pressure, $P(x,y) = P$.

Since none of the boundaries are simply supported, the approximate solution comes from an application of the Rayleigh-Ritz approach. This method in dynamic response problems involves forming the kinetic energy, T, the potential energy, V, and the work done, Q, by the pressure on the plate. The solution for $W(x,y)$ is pursued by minimizing the following equation,

$$T - (V + Q) = \text{stationary value} \tag{15}$$

The kinetic energy is calculated by equation (3).

The potential energy is formed by summing the contributions from the plate bending strain energy and the strain energy in the boundary springs. The bending strain energy can be determined from equation (2). The potential energies associated with the rotational elastic boundary conditions are,

$$V_R = \frac{R_1}{2}\int_o^b W_{,x}^2(o,y)\, dy + \frac{R_2}{2}\int_o^b W_{,x}^2(a,y)\, dy$$

$$+\frac{R_3}{2}\int_0^a W,_y^2(x,o)\ dx + \frac{R_4}{2}\int_0^a W,_y^2(x,b)\ dx \qquad (16)$$

The strain energies associated with the transverse boundary springs are,

$$V_K = \frac{K_1}{2}\int_0^b W^2(o,y)\ dy + \frac{K_2}{2}\int_0^b W^2(a,y)\ dy$$
$$+\frac{K_3}{2}\int_0^a W^2(x,o)\ dx + \frac{K_4}{2}\int_0^a W^2(x,b)\ dx \qquad (17)$$

where all spring coefficients (R_i , K_i (i=1,2,3,4)) are assumed constant along respective edges.

The total potential energy can then be written as,

$$V = V_R + V_K + V_{max,b} \qquad (18)$$

The work done by a uniform pressure field, P , is given as,

$$Q = -P\int_0^a\int_0^b W(x,y)\ dy\ dx \qquad (19)$$

The choice of W(x,y) was given in equation (9) so that the minimization of equation (15) becomes,

$$\frac{\partial_T}{\partial^{A_{mn}}} - \frac{\partial_V}{\partial^{A_{mn}}} = \frac{\partial_Q}{\partial^{A_{mn}}} \qquad (20)$$

Since the response of the plate is ruled by the natural frequencies and geometric mode shapes, the calculation of

natural frequencies is required. This is done by forming the Rayleigh Quotient of equation (4) so that the radian frequency of the mn^{th} mode is given by,

$$\omega_{mn}^2 = \frac{V}{\rho \frac{h}{2} \int_0^a \int_0^b W^2(x,y)\, dy\, dx} \tag{21}$$

where equation (21) can be written as a matrix which is a system of simultaneous equations. The natural frequencies are obtained when the determinant is set to zero. It involves the evaluation of many difficult integrals. For this reason, MACSYMA is very helpful. The evaluation is given in Appendix C.

Combining equations (20) and (21), the minimization problem becomes,

$$\frac{\partial T}{\partial A_{mn}} \left(1 - \frac{\omega_{mn}^2}{\omega^2} \right) = \frac{\partial Q}{\partial A_{mn}} \tag{22}$$

where equation (22) is also a matrix of simultaneous equations which allows the calculation of the constants, A_{mn}, by substitution of equations (3), (9)-(11) and (19). These results are described in Appendix D.

The calculation of the coefficients, A_{mn} , at this point makes the solution for the spatial distribution of displacement, W(x,y), complete.

The resulting strains are then calculated by the small deflection theory as follows,

$$\epsilon_x = - z\, w_{,xx} = - z\, W_{,xx}\, e^{i2\pi ft} \tag{23}$$

and,

$$\epsilon_y = - z\, w_{,yy} = - z\, W_{,yy}\, e^{i2\pi ft} \tag{24}$$

where $2\pi f = \omega$. The maximum strains are calculated at the top and bottom surfaces of the panel at $z=\pm h/2$.

The magnitude of mean-square strains at a frequency, f, are determined by,

$$\overline{\epsilon_x^2} = \frac{1}{2}\epsilon_x \epsilon_x^* = \frac{1}{2}\left|\epsilon_x^2\right| \tag{25}$$

and,

$$\overline{\epsilon_y^2} = \frac{1}{2}\epsilon_y \epsilon_y^* = \frac{1}{2}\left|\epsilon_y^2\right| \tag{26}$$

where * denotes the complex conjugate.

CHAPTER 3

Symbolic Manipulation as an Aid to Solution

Introduction and Description of MACSYMA*

Historically, machine aided mathematics has experienced an arithmetical development. The focus has been to provide a means to process large amounts of information numerically. This is reflected in the widely held desire to statistically evaluate numerical data. As a result, the majority of software systems available are designed for digital data processing. Any analytical relation related to the numbers is usually derived prior to computer use and incorporated into the data processing or the relation is discovered with further numerical evaluation such as curve fitting. The computer has proven to be very capable to perform statistical analysis but the accuracy and efficiency are not always good. Large sets of data require large storage space in the machine and truncation with roundoff is not uncommon.

Since the computer combines and arranges numerical quantities based on mathematical expressions that manipulate variables, parameters or any general symbol, it is not unreasonable to expect these same mathematical expressions

---

* Acronym for MAC's SYmbolic MAnipulation System

to be derivable on the machine. During the execution of an algorithm, the computer need not discriminate between numbers and symbols until the user so specifies with an output request. Research and development of computer aided mathematics is best exemplified by MACSYMA.

MACSYMA's initial development was done under the direction of Professor Joel Moses at Massachusetts Institute of Technology in the latter part of the 1960's (15). Since then, it has become commercially available through Symbolics, Inc. The history of MACSYMA's development shows continuous contributions to improvements and system maintenance by many authors. The system has evolved into a large and sophisticated symbolic manipulation software package that gives the user access to many otherwise unavailable mathematical techniques. This has produced a library of user shared algorithms that have been employed in such fields as experimental mathematics, acoustics, celestial mechanics, computer aided design, structural mechanics and numerical analysis. The types of problems that have been addressed include spectral analysis, helicopter blade motion, finite element analysis and plate vibrations, among many others (16).

MACSYMA is a lisp program (recently estimated at 300,000 lines of lisp code (16)) that has been catalogued to include basic algorithms and axioms of mathematical theory. The growth of MACSYMA is not unlike the evolution of math itself in that advanced theory is dependent on the validity of fundamental assertions. This " building block " process

is apparent in mathematical proofs or derivations whereby any conclusion must logically follow preceding steps of the argument and MACSYMA has experienced this same " building block development. The program has attained a level of sophistication that offers on-screen two-dimensional representations (very similar to handwritten form) of advanced calculus and linear algebra. Accordingly, the program commands for the manipulation of user defined variable expressions are similar to the mathematical functions desired. For example, in order to factor an expression, the MACSYMA syntax is,

factor(expression);

or to expand a rational expression by cancelling a common divisor, multiplying out products of sums, etc, the syntax is,

ratexpand(expression);

or to simplify a trigonometric expression by the implementation of the identity, $\sin^2(x) + \cos^2(x) = 1$, the command is,

trigsimp(expression);

Also, the arithmetical operators used to enter and create equations are the same as those used in many program languages where ** = exponentiation, / = division, etc. As a result, it is not difficult to begin the application of MACSYMA capabilities and subsequent requests are user discovered in a friendly manner.

Perhaps the most valuable asset given by MACSYMA and other available symbolic manipulation software is the release from computational details of problem solutions. Many solution derivations involve long and difficult intermediate calculations where a strong chance for error is present if the computations are done by hand. Even commonly used tables of integrals contain errors. A computer algebra system puts the mathematics of solution in the hands of the practicioner. The answers returned by MACSYMA are given in general form according to the degree of generality requested. This frees an engineer to directly define and apply general solution techniques and algorithms to a class of problems and allows the examination and development of theory from the definitions. The insight to be gained from engineering theory and physical phenomenon is not lost in the details of derivation. Since mathematics is a tool of the engineer, it is advantageous to let the computer assume the role of the analytic work-horse.

Examples of MACSYMA Capabilities

The capabilities of MACSYMA are too numerous to mention all here. Examples, with an emphasis on those related to the current study, include the ability to perform definite and indefinite integration, differentiation, evaluation of limits and series summations, trigonometric and hyperbolic function manipulation as well as matrix and tensor manipulation. The program can also evaluate expressions numerically at intermediate stages and MACSYMA is able to generate fortran code. Collectively, these capabilities provide the means to create

subroutines that can be developed and verified separately. It is also a more efficient use of computer time to simplify expressions prior to numerical evaluation which MACSYMA can perform with variable precision on both fixed and floating point calculations.

In order to illustrate an application of MACSYMA capabilities to problem solution, it is pertinent to present examples of manipulations related to the current study. The examples include the display of MACSYMA generated beam functions and a description of steps necessary to form the Rayleigh quotient for natural frequencies. The Rayleigh quotient is applied to a simply-supported panel utilizing beam sine functions as the assumed mode shapes. The example using sine functions was chosen for presentation because it is not conceptually difficult and gives an easy to follow MACSYMA listing. Both examples have been edited to exclude details of MACSYMA program statements and since MACSYMA exhibits no greek nomenclature, english abbreviations are used. The examples will also introduce the two-dimensional display returned by MACSYMA that is used in Appendices B, C and D.

MACSYMA Generated Beam Functions

The beam functions chosen to represent the modes of vibration of an elastically restrained plate were given in equations (10) and (11). The following brief listing is a demonstration of computer generated expressions for these beam functions. The functions are inserted into equation (9)

and expanded in the series summation for a finite number of terms.

The general expression for the assumed displacement functions from equation (9) is represented by MACSYMA as,

$$w(x, y) = \sum_{n=1}^{q} \left(\sum_{m=1}^{p} x(m)\, a(m, n) \right) y(n) \tag{27}$$

The expressions for $X_m(x)$ and $Y_n(y)$ from equations (10) and (11) are,

$$x(m) = b(m)\, \sinh\left(\frac{alph(m)\, x}{a}\right) + c(m)\, \sin\left(\frac{alph(m)\, x}{a}\right) + d(m)\, \cosh\left(\frac{alph(m)\, x}{a}\right) + \cos\left(\frac{alph(m)\, x}{a}\right) \tag{28}$$

and,

$$y(n) = e(n)\, \sinh\left(\frac{bet(n)\, y}{b}\right) + f(n)\, \sin\left(\frac{bet(n)\, y}{b}\right) + g(n)\, \cosh\left(\frac{bet(n)\, y}{b}\right) + \cos\left(\frac{bet(n)\, y}{b}\right) \tag{29}$$

Substituting equations (28) and (29) into (27),

$$w(x, y) = \sum_{n=1}^{q} \left(\sum_{m=1}^{p} a(m, n) \right) \left(b(m)\, \sinh\left(\frac{alph(m)\, x}{a}\right) + c(m)\, \sin\left(\frac{alph(m)\, x}{a}\right) \right.$$

$$+ d(m)\cosh\left(\frac{alph(m)\,x}{a}\right) + \cos\left(\frac{alph(m)\,x}{a}\right)))$$

$$(e(n)\sinh\left(\frac{bet(n)\,y}{b}\right) + f(n)\sin\left(\frac{bet(n)\,y}{b}\right)$$

$$+ g(n)\cosh\left(\frac{bet(n)\,y}{b}\right) + \cos\left(\frac{bet(n)\,y}{b}\right)) \qquad (30)$$

and finally expanding to show four terms (p=2 , q=2) we have,

$$w(x, y) = (a(2, 2)\,(b(2)\sinh\left(\frac{alph(2)\,x}{a}\right)$$

$$+ c(2)\sin\left(\frac{alph(2)\,x}{a}\right) + d(2)\cosh\left(\frac{alph(2)\,x}{a}\right)$$

$$+ \cos\left(\frac{alph(2)\,x}{a}\right)) + a(1, 2)\,(b(1)\sinh\left(\frac{alph(1)\,x}{a}\right)$$

$$+ c(1)\sin\left(\frac{alph(1)\,x}{a}\right) + d(1)\cosh\left(\frac{alph(1)\,x}{a}\right)$$

$$+ \cos\left(\frac{alph(1)\,x}{a}\right))) (e(2)\sinh\left(\frac{bet(2)\,y}{b}\right)$$

$$+ f(2)\sin\left(\frac{bet(2)\,y}{b}\right) + g(2)\cosh\left(\frac{bet(2)\,y}{b}\right) + \cos\left(\frac{bet(2)\,y}{b}\right))$$

$$+ (a(2, 1)\,(b(2)\sinh\left(\frac{alph(2)\,x}{a}\right) + c(2)\sin\left(\frac{alph(2)\,x}{a}\right)$$

$$+ d(2)\cosh\left(\frac{alph(2)\,x}{a}\right) + \cos\left(\frac{alph(2)\,x}{a}\right))$$

$$+ a(1, 1)\,(b(1)\sinh\left(\frac{\mathrm{alph}(1)\,x}{a}\right) + c(1)\sin\left(\frac{\mathrm{alph}(1)\,x}{a}\right)$$

$$+ d(1)\cosh\left(\frac{\mathrm{alph}(1)\,x}{a}\right) + \cos\left(\frac{\mathrm{alph}(1)\,x}{a}\right)))$$

$$(e(1)\sinh\left(\frac{\mathrm{bet}(1)\,y}{b}\right) + f(1)\sin\left(\frac{\mathrm{bet}(1)\,y}{b}\right)$$

$$+ g(1)\cosh\left(\frac{\mathrm{bet}(1)\,y}{b}\right) + \cos\left(\frac{\mathrm{bet}(1)\,y}{b}\right)) \qquad (31)$$

Simply-Supported Plate Solution-

(MACSYMA), Rayleigh Quotient

The expression for the Rayleigh quotient that is formed from the plate strain and kinetic energies was given in equation (4). Another demonstration of MACSYMA capabilities is provided whereby the integral expressions for the energy terms are computer generated, the quotient is formed and beam functions are inserted. The partial derivatives are evaluated for the strain energy integrand expressions and integration is performed over the plate surface.

The simply-supported plate solution can be represented by sine functions taken from the simply-supported beam. When these functions are used, the equation for natural frequencies reduces to the well known exact expression.

Forming the quotient from equation (4), MACSYMA gives,

$$\mathrm{nfmn}^2_{\mathrm{radian}} = d\left(\int_0^b \int_0^a \left(\frac{d^2}{dy^2}\,(w(x, y))\right)^2\right.$$

$$+ 2\,pr\left(\frac{d^2}{dx^2}(w(x,y))\right)\left(\frac{d^2}{dy^2}(w(x,y))\right) + \left(\frac{d^2}{dx^2}(w(x,y))\right)^2$$

$$- 2\,pr\left(\frac{d^2}{dx\,dy}(w(x,y))\right)^2 + 2\left(\frac{d^2}{dx\,dy}(w(x,y))\right)\,dx\,dy)$$

$$/(h\,rho\int_0^b\int_0^a w^2(x,y)\,dx\,dy)$$

(32)

The normal modes of vibration of a simply-supported plate can be represented by,

$$wmn\,\sin\left(\frac{\%pi\,m\,x}{a}\right)\sin\left(\frac{\%pi\,n\,y}{b}\right) \tag{33}$$

and substituting equation (33) into (32),

$$nfmn^2 \text{ radian} = d$$

$$\int_0^b\int_0^a \left(\frac{d^2}{dy^2}\left(wmn\,\sin\left(\frac{\%pi\,m\,x}{a}\right)\sin\left(\frac{\%pi\,n\,y}{b}\right)\right)\right)^2 (I)$$

$$+ 2\,pr\left(\frac{d^2}{dx^2}\left(wmn\,\sin\left(\frac{\%pi\,m\,x}{a}\right)\sin\left(\frac{\%pi\,n\,y}{b}\right)\right)\right)$$

$$\left(\frac{d^2}{dy^2}\left(wmn\,\sin\left(\frac{\%pi\,m\,x}{a}\right)\sin\left(\frac{\%pi\,n\,y}{b}\right)\right)\right)$$

$$+\left(\frac{d^2}{dx^2}\left(wmn\,\sin\left(\frac{\%pi\,m\,x}{a}\right)\sin\left(\frac{\%pi\,n\,y}{b}\right)\right)^2\right)$$

$$-2\,pr\left(\frac{d^2}{dx\,dy}\left(wmn\,\sin\left(\frac{\%pi\,m\,x}{a}\right)\sin\left(\frac{\%pi\,n\,y}{b}\right)\right)^2\right)$$

$$+2\left(\frac{d^2}{dx\,dy}\left(wmn\,\sin\left(\frac{\%pi\,m\,x}{a}\right)\sin\left(\frac{\%pi\,n\,y}{b}\right)\right)^2\right)dx\,dy)$$

$$/(h\,rho\,wmn^2\left(\int_0^a \sin^2\left(\frac{2\,\%pi\,m\,x}{a}\right)dx\right)\left(\int_0^b \sin^2\left(\frac{2\,\%pi\,n\,y}{b}\right)dy\right)$$

(34)

The respective derivatives are taken and MACSYMA yields,

$$nfmn_{radian}^2 = d$$

$$\left(\int_0^b\int_0^a \frac{2\,\%pi^4\,m^2\,n^2\,pr\,wmn^2\,\sin^2\left(\frac{2\,\%pi\,m\,x}{a}\right)\sin^2\left(\frac{2\,\%pi\,n\,y}{b}\right)}{a^2\,b^2}\right)$$

$$+\frac{\%pi^4\,n^4\,wmn^2\,\sin^2\left(\frac{2\,\%pi\,m\,x}{a}\right)\sin^2\left(\frac{2\,\%pi\,n\,y}{b}\right)}{b^4}$$

$$
\begin{aligned}
&\frac{\%pi^4\ m^4\ wmn^2\ \sin^2\left(\frac{2\,\%pi\,m\,x}{a}\right)\sin^2\left(\frac{2\,\%pi\,n\,y}{b}\right)}{a^4} \\
&+ \frac{2\,\%pi^4\ m^2\ n^2\ pr\ wmn^2\ \cos\left(\frac{2\,\%pi\,m\,x}{a}\right)\cos\left(\frac{2\,\%pi\,n\,y}{b}\right)}{a^2\ b^2} \\
&+ \frac{2\,\%pi^4\ m^2\ n^2\ wmn^2\ \cos\left(\frac{2\,\%pi\,m\,x}{a}\right)\cos\left(\frac{2\,\%pi\,n\,y}{b}\right)}{a^2\ b^2}\ dx\ dy)
\end{aligned}
$$

$$
/(h\ rho\ wmn^2\ (I_0^a \sin\left(\frac{2\,\%pi\,m\,x}{a}\right) dx)\ I_0^b \sin\left(\frac{2\,\%pi\,n\,y}{b}\right) dy) \qquad (35)
$$

and performing the integration,

$$
nfmn^2_{radian} = \frac{d\ (\%pi^4\ a^4\ b^4\ n^4 + 2\,\%pi^4\ a^4\ b^2\ m^2\ n^2 + \%pi^4\ b^4\ m^4)}{a^4\ b^4\ h\ rho^5} \qquad (36)
$$

Finally, a simplification gives,

$$
nfmn^2_{radian} = \frac{\%pi^4\ d\ (a^2\ n^2 + b^2\ m^2)^2}{a^4\ b^4\ h\ rho} \qquad (37)
$$

which is the exact expression.

Considerations to Current Approach

The first consideration to the Rayleigh-Ritz approach attempted herein is the generation of beam functions that display unsymmetric boundary conditions. Although the algebraic manipulations could be done by hand, the intermediate calculations involved are long and cumbersome. Substitution of the general expressions of the beam functions into three of the equations of the boundary conditions involves taking derivatives (first, second and third order) and simultaneous solution for the coefficients, B, C and D. The expressions for these coefficients are then inserted into the fourth boundary equation yielding a transcendental equation for the argument, α . This transcendental equation is solved numerically using the Newton-Raphson method. This requires the derivative with respect to α of that equation. Appendix B displays the lengthy expressions returned by MACSYMA for these calculations. For comparisons of degree of difficulty, the calculations were performed by hand. This comparison is described in chapter six.

Once the beam functions are derived, it is necessary to obtain expressions for the integrals of the energy terms for natural frequencies. Again, these computations could be done by hand, however without symmetric simplifying assumptions, the manipulations are arduous. Carmichael assumed symmetric restraint conditions on parallel edges and was rewarded with concise easy to program results. By examining the necessary integrals with consideration paid to displacement and slope

on those parallel sides, the integrals were reduced to explicit expressions in terms of the coefficients (see reference 13). Unfortunately, the assumption of unsymmetric boundary conditions in this study does not allow the reduction of the integrals to simple expressions. With the aid of MACSYMA, these integrals are directly evaluated over the plate surface resulting in the equations given in Appendix C.

Carmichael demonstrated another simplification when considering the extraction of natural frequencies. By diagonalizing the eigenvalue problem, the mn^{th} mode is represented by the mn^{th} term only. This was an acceptable approximation since the off diagonal terms are much smaller than the diagonal terms in the frequency determinant. As a result, the off diagonal terms make minimal contribution to the calculation of natural frequencies. Carmichael's analysis displayed an error of less than 1% by using this type of approximation. Diagonalization of the frequency determinant is used in this study also to simplify the derivation and programming of solution. Accuracy of the results is shown in chapter five.

Another consideration to the MACSYMA aided solution method relates to the determination of the coefficients, A_{mn}, of forced response. Equation (22) shows the necessary equation for this calculation. It should be noted that equation (22) is for an undamped structure. Damping is incorporated into the computation in Appendix D. The damping term is inserted once the expression for the undamped A_{mn} is found. The equation for these coefficients requires the evaluation of

the integral formed by the work done by the pressure on the plate (equation (19)). Although this integral is not as difficult as those from the plate strain and kinetic energies, MACSYMA again performs the integration conveniently.

As a final note to the determination of the coefficients, a similar diagonalization is made to the simultaneous equations arising from equation (22). Roussos discovered that the off diagonal terms are again small in comparison to the terms on the diagonal (see reference 5). This simplification aids in the programming of the solution algorithm. The accuracy resulting from this assumption is given in chapter five.

CHAPTER 4

Finite Elements as a Solution Method

Introduction and Description of NASTRAN*

Since the early 1960's, the finite element method has had an accelerated development and has gained wide acceptance to many engineering applications. Although it was initially designed to be used in structural analysis, it has been successfully employed in other engineering disciplines such as fluid mechanics and heat transfer. Perhaps the main reason the finite element method has experienced such rapid advancement is the computational power given by the computer.

Essentially, the finite element method (as applied to structural analysis) is an energy formulation similar to the Rayleigh-Ritz approach. However, rather than define admissible functions over the entire domain, functions are chosen to describe the behavior over elements or subdomains. That is, the continuous domain is discretized into a finite number of elements. The functions (called element interpolation functions) are usually easier to define than admissible functions over an entire domain. In fact, low order polynomials are often chosen which facilitates integration of the energy terms. As

---

* Acronym for NASA STRuctural ANalysis Program

a result, the method can be applied to structures of complicated geometry. Once the equations are used to determine the elemental mass matrices, stiffness matrices and force vectors, they are assembled to describe the behavior of the entire structure. Compatibility of displacement is required at the grid points connecting the elements as the global matrices and vectors are assembled. The manipulations of matrix algebra are then used to to retrieve the solution data.

NASTRAN is a comprehensive finite element software package that has been developed with general purpose objectives (17). The program can be used to examine structures of any size, shape and configuration. It will handle structures that exhibit isotropic to generally anisotropic elastic relations. The program is able to perform real or complex matrix operations and determine vibration frequencies and modes. Various loadings may be applied to the structural grid points including concentrated loads and distributed loads. The loads can be transient, sinusoidal steady state and random. Flexibility has been incorporated into the NASTRAN program package in an effort to anticipate changing needs and applications. As described, NASTRAN is quite capable to analyze uniform rectangular plates with elastic restraining springs on the edges. Rectangular plates are conveniently modeled with a cartesian coordinate grid configuration. NASTRAN uses the displacement approach with reference to the grid points to analyze these structures. NASTRAN uses a polynomial representation of the displacements.

A typical NASTRAN analysis involves an input file that is composed of three parts (18). These are the executive control, the case control and the bulk data. The executive control portion defines the type of solution (i.e. static, dynamic, heat transfer, etc.) to be used and estimates the time of computation. Several options for special features such as diagnostic requests are also designated in the executive control.

The case control provides more detail of the input to the specific problem under consideration. The selection of eigenvalue extraction method, the specification of loading cases to be examined and the output frequency selections are made in the case control. Model and material properties such as damping of the structure are referenced and grid point constraints are selected from the bulk data. Requests of type, location and sorting of the output are issued in this section.

The third and most detailed part of the NASTRAN input is the bulk data. This section is a formatted data list that describes the model and material properties. The grid configuration is specified by grid point location and element connectivities. Loading is indicated with amplitude and time or frequency variation as well as points of load application. Parameters that control accuracy of solution are listed. The bulk data is the "meat" of the NASTRAN input and can be a long listing. As a result, it is the bulk data that presents the best chance for format error.

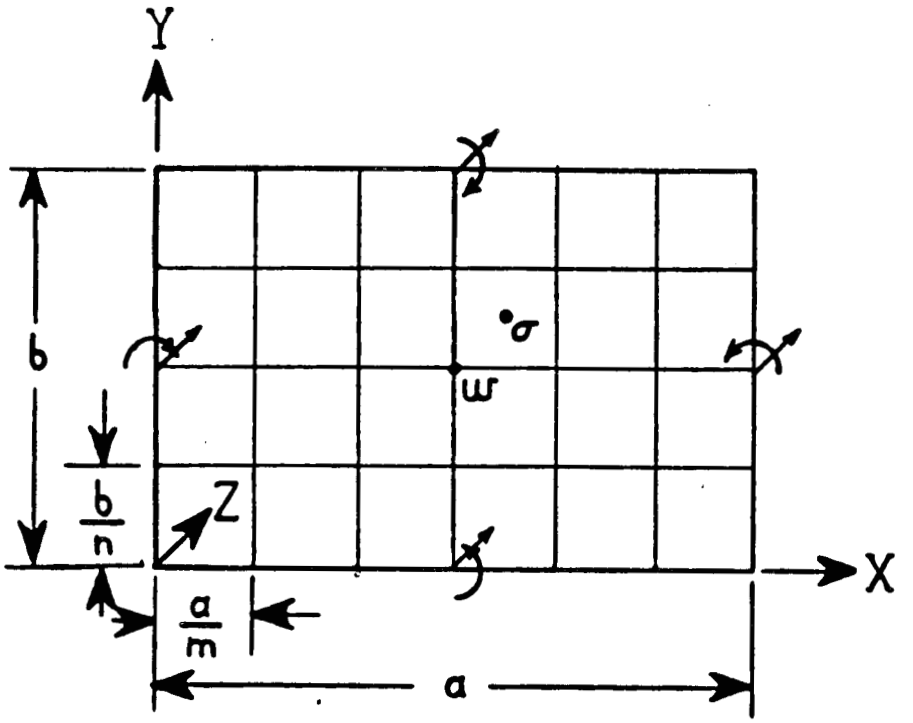

Figure (2). NASTRAN Finite Element Model

Description of Elements and Models

The models (figure (2)) chosen for analysis in this study were composed of isotropic quadrilateral (CQUAD1) elements of uniform thickness. The CQUAD1 element possesses both in-plane and bending stiffnesses although the in-plane motions were neglected since the two motions are uncoupled in small deflection linear transverse vibrations. This element uses two sets of coplanar overlapping bending triangles (figure (3)) that

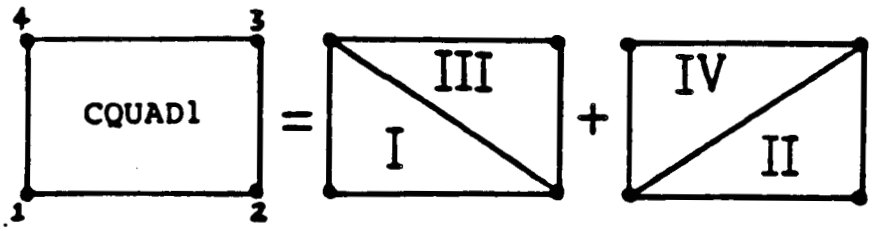

Figure (3). CQUAD1 Element Consisting of Overlapping Pairs of Triangular Plate Elements

each have one half the quadrilateral thickness. Line segments joining points are assumed rigid. The stresses are computed for each triangle at the intersection of the diagonals and averaged (19). For rectangular elements, this calculation is at the center of the element. Strains are not calculated in NASTRAN dynamic analysis. The accuracy returned by the CQUAD1 element is described in reference (19).

The other element necessary is the scalar spring element to model elastic boundary restraints. Scalar spring elements (CELAS1) were attached to each grid point on the four edges of the plates. Two spring elements were fixed to each grid point (one for translation and one rotation). At the corners, however, it was necessary to attach an additional rotational spring in order to model the joining of two respective edges. The connections were completed by fixing each spring from grid point to grounded scalar points. The bulk data was arranged so as to allow the assignment of the eight distinct spring constants (four edges with two types of spring on each edge).

Six models were employed to conduct the study. They included 15"x 3", 15"x 6", 15"x 9", 15"x 12" and two square plates at 12"x 12" and 15"x15". These models gave aspect ratios (=b/a) of 0.2, 0.4, 0.6, 0.8 and 1.0, respectively. The input data given to NASTRAN for each model was representative of the material properties of a typical aluminum panel. Upon retrieval of the output data, the frequencies and responses were nondimensionalized as described in the

results. The analysis was conducted using NASTRAN normal modes frequency response.

Eigenvalue Extraction

Once the global mass and stiffness matrices are assembled, the eigenvalues and eigenvectors are extracted according to the formula,

$$([K] - \lambda[M])\{\phi\} = 0 \tag{38}$$

where, [M] and [K] are the global mass and stiffness matrices, λ and $\{\phi\}$ are the desired eigenvalues and eigenvectors, respectively. The method selected for this extraction was the Inverse Method with Shifts (19). The NASTRAN software package contains the algorithm for this procedure.

The inverse method is a vector iteration procedure. Writing equation (38) as,

$$\{v\}_{n+1} = [D]\{u\}_n \tag{39}$$

where,

$$[D] = [K]^{-1}[M] \tag{40}$$

and $\{u\}_n$ is the trail input vector (arbitrary initial trail vector, $\{u\}_1$) and $\{v\}_{n+1}$ is the vector obtained from the n^{th} iteration.

Then the $n+1^{st}$ trail vector input to the iteration is,

$$\{u\}_{n+1} = \lambda_{(n+1)}\{v\}_{n+1} \tag{41}$$

where $\lambda_{(n+1)}$ is an appropriate scaling factor. NASTRAN selects $\lambda_{(n+1)}$ as the inverse of the element of largest absolute value in $\{v\}_{n+1}$ so as to normalize $\{u\}_{n+1}$ with +1 as the largest element. It has been proven (19) that $\{v\}_{n+1}$ converges to the eigenvector, $\{\phi\}$ and $\lambda_{(n+1)}$ converges on

the corresponding eigenvalue, λ . In most cases, the procedure results in the lowest eigenvalue.

In order to obtain eigenvalues and eigenvectors of higher modes, the algorithm is employed with spectrum shift. That is, a shift point, λ_o is selected that is close to a higher eigenvalue and a shifted eigenvalue is defined as,

$$\Lambda = \lambda - \lambda_o \tag{42}$$

Substituting into equation (38),

$$([K^*] - \Lambda [M]) \{\phi\} = 0 \tag{43}$$

where,

$$[K^*] = [K] - \lambda_o [M] \tag{44}$$

The inverse method is then applied to this shifted eigenvalue problem. Λ is solved for and the required eigenvalue is,

$$\lambda = \lambda_o + \Lambda \tag{45}$$

The convergence criteria used by NASTRAN is based on orthogonality. A check of retrieved eigenvectors is made such that the modal mass matrix,

$$\{\phi_i\}^T [M] \{\phi_j\} < \gamma \quad i=j \tag{46}$$

where γ is a user supplied parameter and in the ideal case, $\gamma = 0$.

Finally, mention should be made about the use of inconsistent (lumped) and consistent mass formulations. The lumped mass formulation assembles mass matrices by lumping equal amounts of mass at the grid points. As a result, the mass matrix is diagonal. This type of simplification tends to lower the extracted eigenvalues similar to the effect of a

larger denominator in the Rayleigh quotient (equation (4)). Although this may seem favorable by the argument of upper bounded eigenvalues, computational accuracy may suffer. The natural frequencies obtained in this formulation converge on the true values from below as the number of elements increases.

In the consistent mass formulation, the off diagonal terms are nonzero. These terms couple the adjacent grid points. The eigenvalues retrieved in this case converge more rapidly with a smaller number of elements.

Inadvertently, initial program runs using NASTRAN were done under the lumped mass conditions. After subsequent checks of the results from NASTRAN employing the consistent mass formulation, it was found that the finite element models had been constructed with a sufficient number of elements for good convergence of natural frequencies of lower modes. All NASTRAN runs were done using consistent mass thereafter.

Loading and Geometric Considerations

To properly distribute the continuous uniform elastic boundary restraints along each edge on the finite element models, equivalent discrete values must be determined. A scalar spring was attached to each edge grid point and values were assigned according to the formula,

$$R_i \text{ or } K_{i\ NASTRAN} = \frac{(R_i \text{ or } K_i \text{ / unit length}) \times \text{side length}}{\text{\# elements along side}} \qquad (47)$$

Figure (4) shows how the values were concentrated at a typical edge grid point. Special consideration was given to the corner points for each respective side which necessitated

the assignment of values equal to one half those from equation (47).

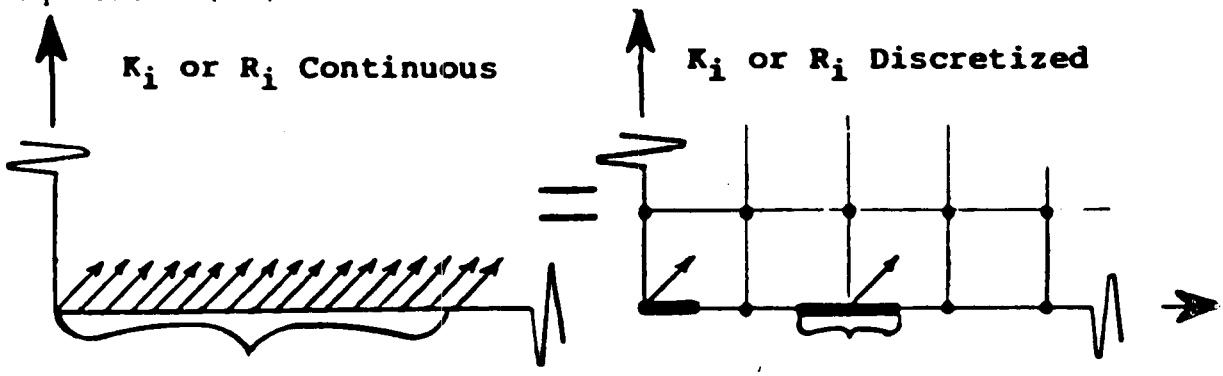

Figure (4).

Similar to the discretized spring values, the uniform pressure load must be divided and concentrated for normal incidence application at every grid point. The equivalent grid point load amplitude values were determined as,

$$P_{NASTRAN} = \frac{(\ P\ /\ \text{unit area}\ )\ x\ \text{total area}}{\text{total \# of elements}} \qquad (48)$$

Figure (5) displays the equivalent geometric application of

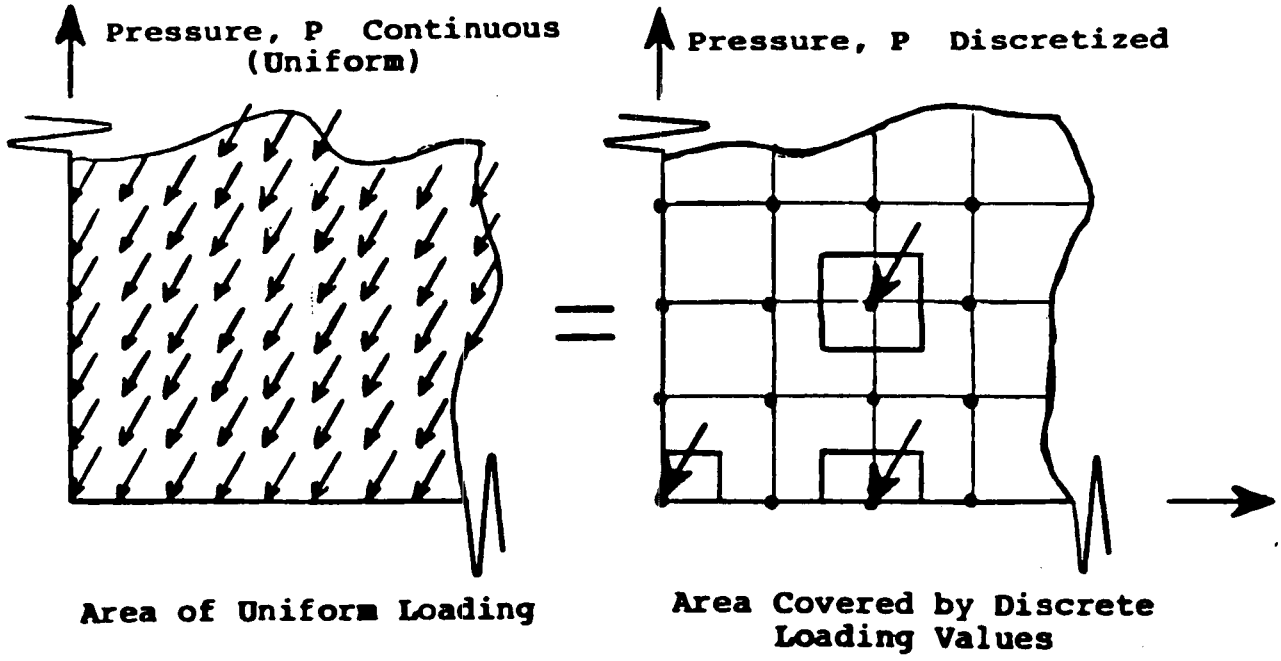

Figure (5).

load at typical grid points. Again, special consideration is required. The edge grid points carried a load amplitude of one half the values from equation (48) and the corner points were assigned 1/4 values.

The accuracy of results returned by this finite element model was previously demonstrated (5).

CHAPTER 5

Results and Comparisons

Frequency and Restraint Parameters

In order to assess the validity of the single term Ritz solution derived using elastically supported beam functions and the results given by NASTRAN, comparisons are now made to frequency parameter studies presented in the literature under various selected edge conditions and aspect ratios. There is a vast amount of literature available on the determination of frequency for the classical simply-supported, clamped and free boundary conditions and the 21 possible combinations from the mixing of these three among the four edges. In general, those cases are considered special limiting cases for the current study. Mainly, comparisons are made to the published results that address the problem of elastically restrained plates as most have been shown to converge on accepted values of frequency for the classical cases. Therefore, the classical edge conditions are noted only as they occur in the limiting case.* The available literature on vibration of plates with elastic restraints is sparse, however, especially for plates possessing both translational and rotational springs at the boundaries.

---

* Numerical values for zero and infinite spring stiffness used in this study were 10^{-4} and 10^{+6}, respectively.

So that the results may be generalized and considered for all uniform isotropic panels, the frequency and restraint parameters are non-dimensionalized according to the formulas given by Warburton and Edney (12). The dimensionless frequency parameter is defined as,

$$\Omega = \omega\, b^2 \sqrt{\rho\, n/D} \tag{49}$$

and the rotational and translational restraint parameters are given as,

$$\begin{aligned} R^* &= Rb/D \qquad x=o,a \\ &= Ra/D \qquad y=o,b \end{aligned} \tag{50}$$

$$\begin{aligned} K^* &= Kb^3/D \qquad x=o,a \\ &= Ka^3/D \qquad y=o,b \end{aligned} \tag{51}$$

The method given by Carmichael (13) is generally regarded as an acceptable Ritz approximation to determine natural frequencies for the cases when edges are between simply-supported and clamped (ie. K=inf as R varies). Table (1) shows the comparison of frequency for selected values of restraint. The first three modes at three values of restraint parameter for five aspect ratios are displayed. It is seen that the new elastic Ritz approximation tends to default to Carmichael's results to within 1%. The discrepancy between the finite element solution and the results of both Ritz solutions is slightly greater and tends to increase as the aspect ratio decreases. The maximum percent difference is 7% occurring at an aspect ratio of 0.2.

Figure (6) shows the variation of fundamental frequency parameter for a square plate as both types of restraint vary from values of zero and infinity as given by Warburton and

Comparison of Characteristic Frequency Parameter
$K_1=K_2=K_3=K_4=$ inf, $R_1=R_2=R_3=R_4=R$

b/a	Rb/D	mode 1	mode 2	mode 3	
1.0	0	19.74	49.35	78.96	*
		19.74	49.35	78.95	**
		19.56	48.90	76.64	***
	20	31.16	64.52	96.17	*
		31.16	64.52	96.15	**
		30.89	64.17	94.66	***
	inf	36.11	73.74	108.90	*
		36.09	73.71	108.81	**
		35.76	73.44	106.79	***
0.8	0	16.19	35.14	45.79	*
		16.19	35.13	45.79	**
		16.03	34.81	45.63	***
	20	25.86	46.17	60.16	*
		25.73	46.30	60.29	**
		25.48	45.96	59.92	***
	inf	29.18	52.76	68.80	*
		29.98	52.75	68.78	**
		29.89	52.13	70.61	***
0.6	0	13.42	24.08	41.03	*
		13.42	24.08	41.84	**
		13.33	23.67	41.21	***
	20	22.34	32.68	50.63	*
		21.84	32.53	50.86	**
		21.26	31.88	50.51	***
	inf	25.97	37.43	57.20	*
		25.96	37.42	57.17	**
		25.98	36.76	56.35	***
0.4	0	11.45	16.19	24.08	*
		11.45	16.18	24.08	**
		11.44	15.97	23.45	***
	20	20.33	24.20	31.26	*
		20.42	24.54	31.98	**
		20.88	24.81	32.92	***
	inf	23.70	27.91	35.56	*
		23.68	27.90	35.53	**
		23.89	28.06	35.59	***
0.2	0	10.26	11.45	13.42	*
		10.26	11.44	13.41	**
		10.38	11.92	14.43	***
	20	19.39	20.17	21.54	*
		19.39	20.22	21.67	**
		19.71	21.34	22.98	***
	inf	22.66	23.49	24.92	*
		22.59	23.42	24.85	**
		23.14	24.86	25.62	***

* Carmichael (Ref.13)
** Ritz Solution herein
*** Nastran F.E. models

Table (1)

Edney. All boundaries are subject to equal restraint. The curve labeled R* =S and K* =inf shows variation from simply-supported to clamped edges and the lowest curve marked R* =0 and K =S displays the changes between the limiting free and simply-supported boundary conditions. Intermediate to these two curves (marked R* =S and K* =S) is the change in frequency

as the edges of the plate vary from free to clamped conditions as both rotational and transverse boundary stiffnesses are increased simultaneously. As stated previously, the assumed displacement functions used by Warburton and Edney consisted of a weighted summation of beam functions displaying the simply-supported, clamped, free and sliding end conditions.

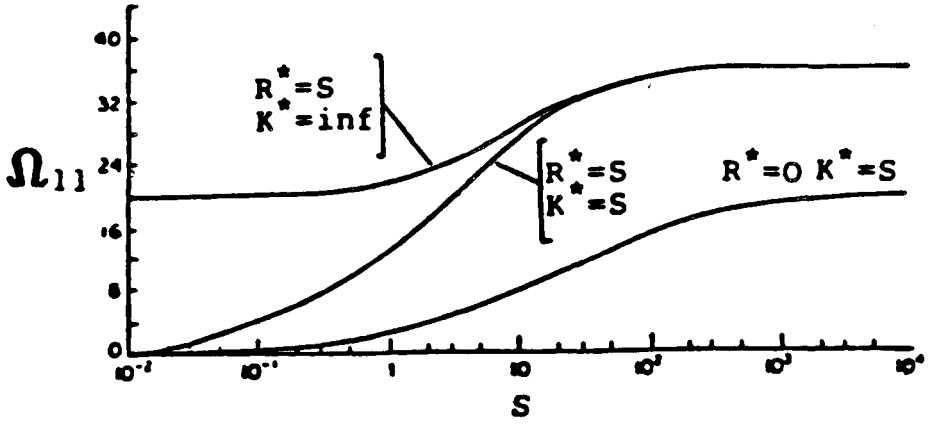

Figure (6). Variation of fundamental frequency parameter Ω_{11} of a square plate with translational and rotational restraint parameters. Identical boundary conditions on all edges. (Taken from reference (12)).

In comparison, figure (7) displays the same study of variation of fundamental frequency as returned by the Ritz solution assuming beam displacement functions that satisfy the general elastic edge conditions and results given by the NASTRAN finite element solution. The top and bottom curves, corresponding to changes in one type of boundary spring while the other is held constant, show good agreement to the results of figure (6). Indeed, the results of all upper and lower curves agree to within 1% for both figures. The intermediate curve of figure (7), however, displays a notable discrepancy when compared to figure (6). The elastic Ritz and finite element solutions agree to within 5% but both return decidedly

lower values of frequency for all values of S on the middle curve except for the limiting cases of the free and clamped boundary conditions.

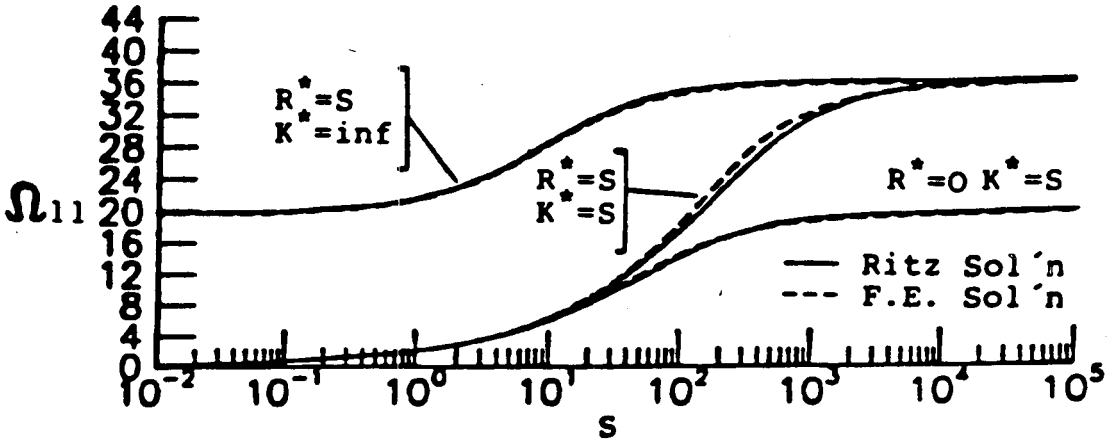

Figure (7). Variation of fundamental frequency parameter Ω_{11} of a square plate with translational and rotational restraint parameters. Identical boundary conditions on all edges.

Returning to discrete numerical comparisons, Filipich, Reyes and Rossi (6) tabulated various fundamental frequency results for selected values of rotational and translational restraint. They assumed functions given by,

$$W(x,y)= \sum_{i=1}^{6} c_i\, x_i\, y_i \qquad (52)$$

where,

$$x_i = \alpha_i\, x^4/a^4 + \beta_i\, x^2/a^2 + 1 \qquad (53)$$

and,

$$y_i = \cos(m_i\, y/b) \qquad (54)$$

and the computations were executed using the Galerkin method. Table (2) shows these results for the case of equal rotational restraint on all edges for a square plate while the transverse edge restraint is held to infinity. This case corresponds to the top curves of figures (6) and (7). For further comparison,

the results given by Mukhopadhyay (7) who used a semi-analytic solution method by applying rotationally restrained beam functions in one coordinate direction and a finite difference approximation in the other direction. The limiting simply-supported and clamped frequency parameter values from Leissa (11) are also included. Table (2) shows general agreement between all solutions, however a maximum percent difference of 10.5% exists between the results of references (6) and (7). The elastic Ritz solution and the finite element results differed from all by no more than 5%.

Comparison of fundamental frequency parameter
Square plate
$K_1=K_2=K_3=K_4=inf$ $R_1=R_2=R_3=R_4=R$

Rb/D	inf	100	10	1	0.1	0	
Ω_{11}	36.01	35.33	31.10	22.90	20.13	19.74	*
	35.99^	34.75		20.51	19.84	19.74^	**
	36.09	34.78	29.55	21.51	19.94	19.74	***
	35.76	34.46	29.32	21.32	19.75	19.56	****

* Filipich, Reyes & Rossi (Ref. (6))
** Mukhopadhyay (Ref. (7))
*** Ritz Solution herein
**** Nastran F.E. Solution
^ Leissa (Ref. (11))

Table (2)

Table (3) gives results that correspond to the curve marked R* =0 and K* =S on figures (6) and (7). Although there was good agreement demonstrated on the lower curves of those graphs, the numerical data of table (3) yields a discrepancy of as much as 50% between the Galerkin method of reference (6) and the two solutions used in this study. Oddly, Warburton and Edney only mentioned the comparative results stating qualitatively that there was good agreement between their results and those of Filipich, Reyes and Rossi. No numerical

data was given to substantiate the statement. Again, the agreement between the elastic Ritz and finite element solutions for this case is to within 1% and the closeness of these results to those of Warburton and Edney for $R^* = 0$ and $K^* = S$ is seen on the bottom curve of figures (6) and (7).

Comparison of fundamental frequency parameter
Square plate
$R_1=R_2=R_3=R_4=0$ $K_1=K_2=K_3=K_4=K$

Kb^3/D	inf	1000	100	10	1	0	
Ω_{11}	19.74	19.55	18.21	11.38	5.92	0	*
	19.74	18.93	14.08	5.97	1.98	0	**
	19.56	18.59	14.44	5.99	1.99	0	***

* Filipich, Reyes & Rossi (Ref. (6))
** Ritz Solution herein
*** Nastran F.E. Solution

Table (3)

As a final example of equal restraint on all of the four edges, the rotational restraining springs are held at infinite stiffness rather than zero shown in table (4). The transverse edge restraint is allowed to vary and the fundamental frequency parameter is tabulated for selected values. This case may be considered as a sliding boundary on foundation springs. The results display a similar disagreement of frequency between the Galerkin solution and the two solutions of this treatise. Filipich, Reyes and Rossi achieved frequency calculations that were higher than the elastic Ritz and finite element results with a 60% discrepancy at $K^* = 10$. As before, the elastic Ritz and NASTRAN results were in close agreement with no more than 5% difference noted.

Tables (5), (6) and (7) address the cases where parallel sides of a square plate are restrained to the same degree. The

Comparison of fundamental frequency parameter
Square plate
$R_1=R_2=R_3=R_4=inf$ $K_1=K_2=K_3=K_4=K$

Kb^3/D	inf	1000	100	10	1	0	
Ω_{11}	36.01	35.33	30.36	16.10	5.60	0	*
	36.09	31.52	17.55	6.24	1.99	0	**
	35.76	32.35	18.31	6.27	1.99	0	***

* Filipich, Reyes & Rossi (Ref. (6))
** Ritz Solution herein
*** Nastran F.E. Solution

Table (4)

solutions used for comparison and the variations of boundary spring parameter are similar as for tables (2), (3) and (4), respectively. First, the transverse edge restraint is held to infinite stiffness as changes are made to the rotational restraint. The variations of fundamental frequency are displayed in table (5). The results of the top row correspond to the case where one pair of opposite edges are clamped while the rotational restraint on the remaining parallel sides is relaxed to converge on the case of opposite sides clamped and the remaining boundaries are simply-supported. An exact value results when parallel edges are simply-supported and is taken from reference (11) for comparison. The bottom row of table (5) shows the variation of frequency as two opposite boundaries are held at the R=0 (simply-supported) value and the remaining two sides change from the clamped (R=inf) to the simply-supported condition. All solutions show good agreement and display at most 3% difference.

Presented in table (6) is the variation of frequency as parallel edges are changed from simply-supported to free end conditions. The rotational restraint is set to zero and the transverse boundary spring is allowed to vary numerically

Comparison of fundamental frequency parameter
Square plate
$K_1=K_2=K_3=K_4=inf \quad R_1=R_2=R_y \quad R_3=R_4=R_x$

$R_y b/D=inf$ $R_x b/D$	inf	100	10	1	0.1	0	
Ω_{11}	36.01	35.67	33.43	29.46	28.97	28.96	*
	35.99^	34.71		28.80	28.22	28.95^	**
	36.09	35.45	32.49	29.61	29.05	28.99	***
	35.76	35.12	32.23	29.39	28.85	28.77	****
$R_y b/D=0$ $R_x b/D$	inf	100	10	1	0.1	0	
Ω_{11}	28.96	28.54	26.03	21.38	19.94	19.74	*
	28.95^	28.23		20.65	19.84	19.74^	**
	28.99	28.21	25.53	20.64	19.84	19.74	***
	28.77	27.99	25.33	20.46	19.66	19.56	****

* Filipich, Reyes & Rossi (Ref. (6))
** Mukhopadhyay (Ref. (7))
*** Ritz Solution herein
**** Nastran F.E. Solution
^ Leissa (Ref. (11))

Table (5)

from infinity to zero. The elastic Ritz solution shows a more rapid descent than either the Galerkin solution of reference (6) or the NASTRAN frequency predictions. Intermediate to the limiting cases of all edges simply-supported or free is the case of opposite sides free while the other parallel edges are simply-supported. This case has an exact value and is given by Leissa (11) as 9.6314. Although the values of the elastic Ritz and Galerkin solutions tend to converge on this, the finite element solution gives an inflated value with a percent difference of 76%. Convergence of the NASTRAN results is exhibited for only cases of equal restraint on all edges in table (6).

For the study shown in table (7), the rotation on the sides is completely constrained (ie. R=inf) while the translational boundary restraint is changed for equal values on parallel edges between infinity and zero. The results show

good agreement between the elastic Ritz and finite element solutions, however both are much lower than the results of reference (6).

Comparison of fundamental frequency parameter
Square plate
$R_1=R_2=R_3=R_4=0$ $K_1=K_2=K_y$ $K_3=K_4=K_x$

$K_y b^3/D=\inf$ $K_x b^3/D$	inf	1000	100	10	1	0[1]	
Ω_{11}	19.74	19.66	18.91	14.76	10.57	9.642	*
	19.74	19.33	16.54	11.31	10.03	9.676	**
	19.56	19.03	17.77	17.09	16.99	16.98	***
$K_y b^3/D=0$ $K_x b^3/D$	inf[1]	1000	100	10	1	0	
Ω_{11}	9.642	9.49	9.39	8.01	3.93	0	*
	9.676	9.48	8.28	4.14	1.43	0	**
	16.98	15.91	11.08	4.34	1.41	0	***

* Filipich, Reyes & Rossi (Ref. (6))
** Ritz Solution herein
*** Nastran F.E. Solution
! SS-Fr-SS-Fr Case, Value from Leissa (Ref. (11)) = 9.6314

Table (6)

Comparison of fundamental frequency parameter
Square plate
$R_1=R_2=R_3=R_4=\inf$ $K_1=K_2=K_y$ $K_3=K_4=K_x$

$K_y b^3/D=0$ $K_x b^3/D$	inf	1000	100	10	1	0	
Ω_{11}	22.39	22.15	20.15	11.38	3.96	0	*
	22.37	20.55	12.38	4.42	1.44	0	**
	22.94	21.02	13.24	4.44	1.41	0	***

* Filipich, Reyes & Rossi (Ref. (6))
** Ritz Solution herein
*** Nastran F.E. Solution

Table (7)

Tables (8), (9) and (10) display comparisons of characteristic frequency parameter for selected cases given by Mukhopadhyay when edges are restrained to different degrees. The boundaries of the plate are completely constrained in the transverse direction (ie. K=inf). As such, edge conditions lie between the simply-supported and clamped states. Each of the tables presents results for plates with boundary springs

on only one side at x=a (ie. side marked 2 on figure (1)). The remaining three sides are held at either the clamped or simply-supported condition. Frequency results are given for four modes at three values of restraint parameter. The aspect ratios selected are for b/a=1.0, 2.5 and 0.4. The ratio of 2.5 was chosen since, for the cases of unsymmetric boundary restraints, natural frequency is dependent on the magnitude of restraint and the side length upon which it is applied. This ratio was achieved by interchanging the x and y coordinate axes on the plate with b/a=0.4.

In table (8), three sides of the panel are held at the simply-supported state while the fourth edge is subject to elastic rotational support. Three select values of restraint parameter are displayed. The agreement of comparison of results of reference (7) are good, in general. The NASTRAN finite element solution gives slightly lower values for all cases other than the first mode at b/a=0.4. The elastic Ritz solution agrees more closely with the results of Mukhopadhyay. The maximum percent difference noted is 3%.

For the cases presented in table (9), three of the sides are clamped as the fourth edge is restrained elastically in rotation. Again, the results of all solutions show general agreement, however for higher modes at b/a=2.5, the elastic Ritz and finite element frequencies are higher than those of reference (7). The maximum percent difference is found there and is approximately 4%.

Comparison of Characteristic Frequency Parameter
$K_1=K_2=K_3=K_4=inf$ $R_1=R_3=R_4=0$ $R_2=R$

b/a	Rb/D	mode 1	mode 2	mode 3	mode 4	
1.0	0.001	19.46	49.21	49.35	79.88	*
		19.74	49.35	49.36	78.95	**
		19.56	48.90	48.91	77.65	***
	1.0	20.19	49.32	50.15	79.43	*
		20.19	49.54	50.09	79.42	**
		20.00	49.08	49.67	78.12	***
	100.0	23.60	51.30	57.21	85.89	*
		23.44	51.77	57.75	85.39	**
		23.17	50.85	57.57	84.91	***
2.5	0.001	71.66	101.33	150.04	219.57	*
		71.55	101.16	150.49	219.57	**
		71.51	100.02	147.12	214.18	***
	1.0	76.30	104.73	152.41	218.36	*
		73.57	102.60	151.48	220.25	**
		73.55	101.49	148.14	214.90	***
	100.0	102.31	127.08	170.99	233.99	*
		99.73	124.48	169.24	235.01	**
		100.15	124.01	166.32	229.42	***
0.4	0.001	11.39	16.16	24.11	35.24	*
		11.45	16.19	24.08	35.13	**
		11.44	16.01	23.54	34.27	***
	1.0	11.42	16.22	24.21	35.35	*
		11.51	16.32	24.29	35.39	**
		11.49	16.13	23.75	34.56	***
	100.0	11.67	17.06	25.70	37.51	*
		11.81	17.17	25.81	37.62	**
		11.71	16.91	25.25	36.95	***

* Mukhopadhyay (Ref. (7))
** Ritz Solution herein
*** Nastran P.E. Solution

Table (8)

Table (10) gives results for the case of a plate possessing clamped boundary conditions on two adjacent edges. one of the remaining edges is simply-supported and the last is elastically restrained in rotation. The results show similar agreement as tables (8) and (9). It is noted that the elastic Ritz and NASTRAN solutions give frequencies that are not consistently higher or lower but may be either. The maximum percent difference is approximately 6%.

The final comparison of frequency is given in table (11). Since no data is available in literature for unsymmetric elastic boundary conditions with both translational and rotational springs, these results compare only the elastic

Ritz and NASTRAN finite element solutions. The fundamental frequency parameter is tabulated for selected values of restraint for a square plate. The rotational and translational dimensionless restraint parameters are held equal in magnitude at 200. Edges are clamped unless specified with restraining values. Except for the case of all edges clamped, the finite element frequency prediction is higher than the elastic Ritz results. The agreement of the two is generally good, however an 8.4% difference is seen for the case of parallel edges elastically restrained with the remaining two boundaries clamped.

Comparison of Characteristic Frequency Parameter
$K_1=K_2=K_3=K_4=inf$ $R_1=R_3=R_4=inf$ $R_2=R$

b/a	Rb/D	mode 1	mode 2	mode 3	mode 4	
1.0	0.001	31.51	63.09	69.33	99.42	*
		31.96	63.65	71.40	101.22	**
		31.60	62.82	71.33	100.34	***
	1.0	31.94	63.83	69.52	99.87	*
		32.36	64.38	71.52	101.68	**
		32.02	63.59	71.49	100.81	***
	100.0	35.43	71.65	72.16	106.08	*
		35.77	72.65	73.45	107.85	**
		35.43	72.32	73.22	106.88	***
2.5[1]	0.001	106.91	138.52	190.11	259.49	*
		107.46	140.37	195.21	271.79	**
		107.35	138.98	192.43	269.36	***
	1.0	112.05	142.42	192.95	261.58	*
		109.66	141.96	196.25	272.43	**
		109.59	140.68	193.63	270.24	***
	100.0	145.25	170.98	216.53	281.25	*
		142.13	168.80	217.06	288.40	**
		143.15	169.36	216.84	288.77	***
0.4	0.001	22.25	25.85	32.69	43.12	*
		23.48	27.06	33.87	44.28	**
		23.69	27.29	33.93	44.16	***
	1.0	22.27	25.89	32.77	43.22	*
		23.49	27.16	34.05	44.52	**
		23.72	27.39	34.11	44.43	***
	100.0	22.45	26.57	34.14	45.28	*
		23.67	27.85	35.41	46.65	**
		23.88	28.02	35.48	46.79	***

* Mukhopadhyay (Ref. (7))
** Ritz Solution herein
*** Nastran F.E. Solution

[1] aspect ratio (b/a)=2.5 achieved by interchanging x and y

Table (9)

Comparison of Characteristic Frequency Parameter
$K_1=K_2=K_3=K_4=inf \quad R_1=R_3=inf \quad R_4=0 \quad R_2=R$

b/a	Rb/D	mode 1	mode 2	mode 3	mode 4	
1.0	0.001	26.84	58.88	60.59	91.69	*
		27.21	61.01	61.02	93.13	**
		26.81	60.19	60.49	90.31	***
	1.0	27.35	59.09	61.36	92.21	*
		27.68	61.15	61.76	93.62	**
		27.31	60.51	61.17	90.82	***
	100.0	31.31	61.41	70.05	99.04	*
		31.59	63.37	70.32	100.23	**
		31.23	62.56	70.18	99.08	***
2.5!	0.001	105.43	133.17	181.15	240.41	*
		105.73	133.99	183.53	254.55	**
		105.73	133.12	180.59	250.14	***
	1.0	110.67	137.32	182.24	242.75	*
		107.97	135.67	184.66	255.26	**
		108.02	134.89	181.87	251.07	***
	100.0	144.09	166.76	208.55	270.01	*
		140.84	163.54	206.61	272.21	**
		143.89	164.45	206.19	270.62	***
0.4	0.001	16.29	21.11	29.24	40.11	*
		16.91	21.44	29.36	40.72	**
		16.92	21.29	28.89	40.02	***
	1.0	16.41	21.24	29.88	40.93	*
		16.94	21.56	29.57	40.98	**
		16.95	21.42	29.10	40.31	***
	100.0	16.69	21.85	30.53	42.55	*
		17.18	22.40	31.11	43.27	**
		17.16	22.18	30.65	42.85	***

* Mukhopadhyay (Ref. (7))
** Ritz Solution herein
*** Nastran F.E. Solution

! aspect ratio (b/a)=2.5 achieved by interchanging x and y

Table (10)

Comparison of Fundamental Frequency Parameter
Square Plate

$R_i^*=R_i b/D \quad K_i^*=K_i b^3/D$

$R_1^*=K_1^*$	$R_2^*=K_2^*$	$R_3^*=K_3^*$	$R_4^*=K_4^*$	Ω_{11}	
200.0	200.0	200.0	200.0	22.13	$
				23.46	$$
200.0	200.0	200.0	inf	24.02	$
				25.07	$$
200.0	inf	200.0	inf	26.02	$
				27.94	$$
200.0	200.0	inf	inf	28.35	$
				30.73	$$
200.0	inf	inf	inf	32.37	$
				33.82	$$
inf	inf	inf	inf	36.09	$
				35.76	$$

$ Ritz Solution herein
$$ Nastran F.E. Solution

Table (11)

Displacement, Acceleration and Strain

The response calculations necessary for design and control of flexible structures is not limited to frequency prediction. Although discrepancies exist between all methods used to predict frequency and academic agreement on an accepted numerical or analytical approach and results can take years, the practicing engineer needs prediction methods for measurable physical response such as displacement, acceleration and strain in order to compare with testing and real applications. Of course it is unreasonable to compare physical response given by a method under any dynamic load if the frequency predictions are unrealistic or disagree. To this end, sample comparisons of the physical responses are now given.

It was stated earlier that the loading is assumed to be a series of harmonic inputs to the mechanical system. The additional assumption of linear small deflection plate theory allows the use of superposition. That is, if the loading can be represented by a harmonic series, the response from each term in the series may be calculated individually and summed over the series for total response. This summation can also be carried out separately for contributions to total response from otner modes of vibration that may be excited. However, the fundamental mode is the easiest to excite and fundamental response makes the major contribution to overall response. This is not to say that the contribution from higher modes should not be considered, but in many cases, it can safely be neglected. For the results presented, loading is taken as

a spatially uniform discrete sinusoidal pressure with a frequency equal to the fundamental frequency of the plate. The single mode harmonic steady-state responses for displacement, acceleration and strain are given. Each of these responses is inversely proportional to structural damping. That is, if damping is doubled, the response is cut in half. The damping used in this study is 5% critical damping.

The solution of steady state harmonic response of a rectangular plate subject to a uniform pressure loading given by the MACSYMA aided elastic Ritz formulation is continuous. The root mean square displacement, acceleration and strain expressions represent a continuous distribution over the plate domain. By specifying coordinates of interest, these response quantities can be examined anywhere on the plate. As well, the strain may be calculated through the panel thickness with the specification of the z coordinate. The assumption of linear plate theory and the absence of shear deformation give a linear distribution of strain through the thickness. Maximum values of strain are found at the top and bottom surfaces of the plate since linear theory assumes that the midplane of the panel is the neutral surface of zero stress/strain. The top and bottom surface strain values are of equal magnitude.

The finite element formulation of NASTRAN does not give a continuous distribution of response quantities. Since the domain is divided into discrete subdomains, the distribution of these numerical quantities is discontinuous. The

displacement and acceleration responses are calculated at nodal points at the corners joining elements while the stresses are obtained from the center of the rectangular quadrilateral elements. These stresses are assumed constant over the element. The linear distribution of stress through the thickness of the plate is retained by NASTRAN, however.

In order to make fair comparisons of response between the elastic Ritz and NASTRAN results, the plate domain was discretized on the finite element models using a cartesian mesh configuration. This configuration places a node point exactly at the center of the plate enabling direct comparison of center displacement and acceleration. Without mesh refinement, center stress is not directly calculated by NASTRAN. Instead, comparisons are made at a point in the center of an element nearest the plate center. The strain calculations done using the elastic Ritz formulation are adjusted to coincide with the coordinates of this near center point on the models. Reference to figure (2) on page 39 clarifies the location of these points.

It was stated earlier that NASTRAN dynamic analysis does not calculate strain. Stresses are returned from calculations requested on a given element. For comparison, these stresses are converted to strains assuming plane stress by the formulas,

$$\epsilon_x = (\sigma_x - \mu\sigma_y)/E \qquad (55)$$

$$\epsilon_y = (\sigma_y - \mu\sigma_x)/E \qquad (56)$$

Upon retrieval of the responses from both methods of solution, the displacement, acceleration and strain values are non-dimensionalized. This is done for general comparison to all isotropic uniform rectangular plates subject to a uniform sinusoidal pressure load at the fundamental frequency. The dimensionless displacement is given by,

$$w_c^* = (D\ w_c)/(P\ b^4) \tag{57}$$

and the dimensionless acceleration is,

$$a_c^* = (D\ a_c\ h)/(P\ b^4\ g) \tag{58}$$

and finally the null-dimensional strain can be given by,

$$\epsilon_c^* = (2\ D\ (1+\mu)\ \epsilon_c)/(h\ P\ b^2) \tag{59}$$

Figures (8) through (13) may best be interpreted by referring to figure (7). The comparison of central pnysical responses is given in the following figures for fundamental resonance excitation of a square plate with identical boundary conditions on all edges. These graphs may be considered crossplots of the displacement, acceleration and strain as they relate first to the boundary restraint values and second to the corresponding changes in fundamental frequency. The three zones as given in figure (7) are also marked on figures (8) through (13). In order to distinguish between the zones marked $R^*=S\ K^*=inf$ and $R^*=0\ K^*=S$, the transition point is noted as the frequency of the simply-supported frequency, Ω_{ss}. Figures (9) and (12) were separated into individual graphs according to the zones for clarity.

The results displayed in figures (8) and (9) show comparison of center displacement between tne single mode elastic

Ritz and the NASTRAN finite element solutions. First, figure (8) gives the variation of displacement with respect to restraint parameter. As expected, the center displacement increases as the elastic restraints are relaxed. In figure (9), the displacement is crossplotted against the range of fundamental excitation frequencies encountered from the restraint relaxation. These two figures taken together show how center displacement varies over the entire domain given in figure (7). There is very good agreement between the elastic Ritz and NASTRAN finite element solutions as seen on the graphs. The results have been truncated at $w_c^*=10^1$ since these approach displacement values outside the region that is normally considered as small deflection.

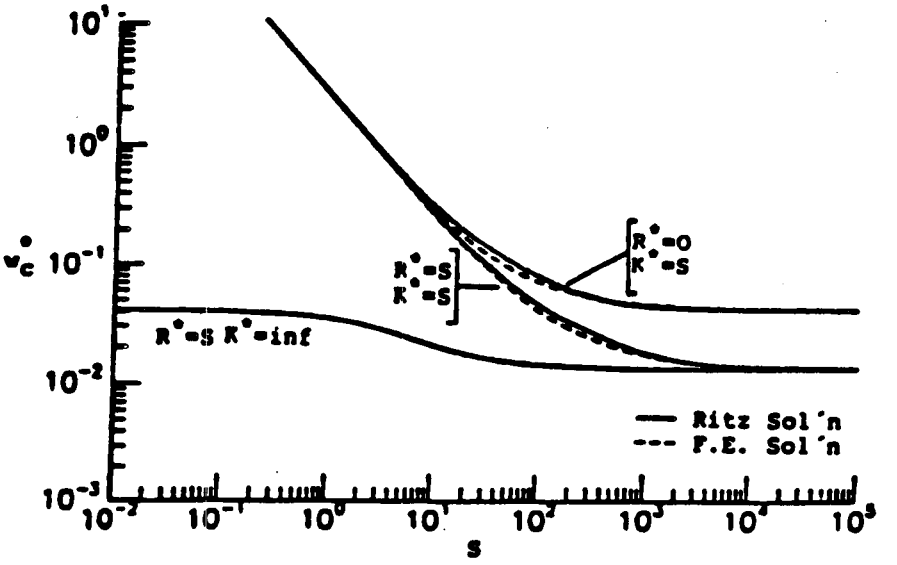

Figure (8). Variation of center displacement with respect to restraint parameter, S, of a square plate with translational and rotational restraint parameters. Identical boundary conditions on all edges. Sinusoidal load at fundamental frequency, f_{11}.

Figures (10)and (11) show the same type of crossplots for center acceleration. Good agreement between the NASTRAN

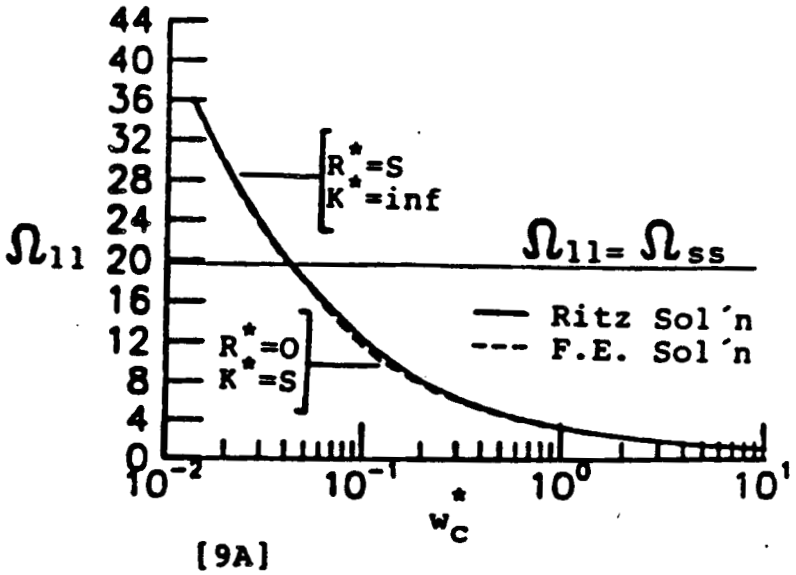

[9A]

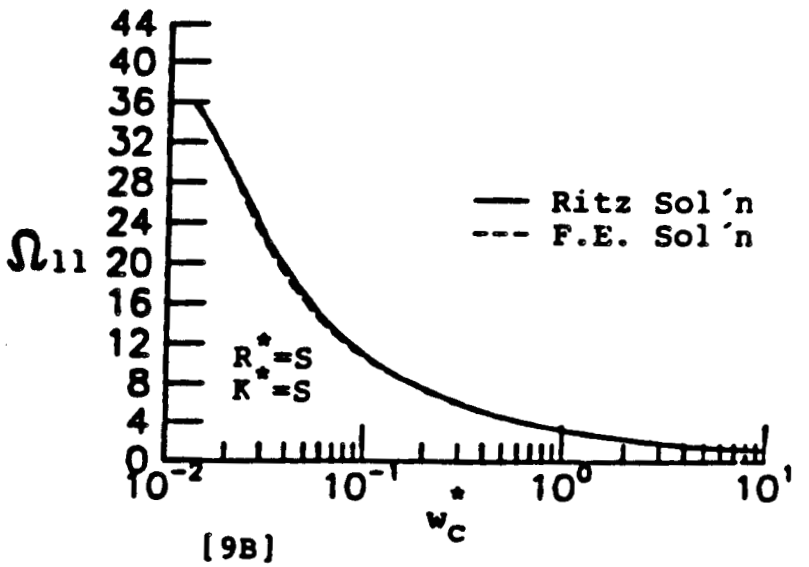

[9B]

Figure (9). Variation of center displacement with respect to fundamental frequency parameter, Ω_{11}, of a square plate with translational and rotational restraint parameters. Identical boundary conditions on all edges. Sinusoidal load at fundamental frequency, f_{11}.

and elastic Ritz results is again seen and may be expected since the frequency and displacement predictions were in close agreement. The magnitude of acceleration can be calculated by multiplying radian frequency squared times the displacement magnitude. Therefore, acceleration calculations

reflect a type of combined error for frequency and displacement computations.

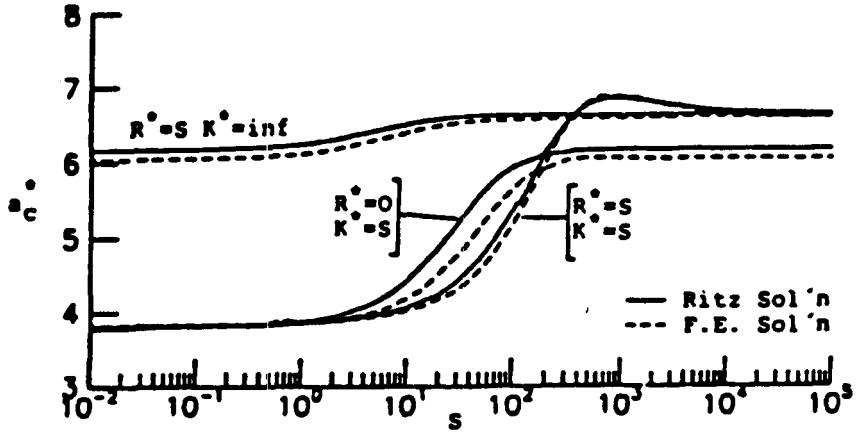

Figure (10). Variation of center acceleration with respect to restraint parameter, S, of a square plate with translational and rotational restraint parameters. Identical boundary conditions on all edges. Sinusoidal load at fundamental frequency, f_{11}.

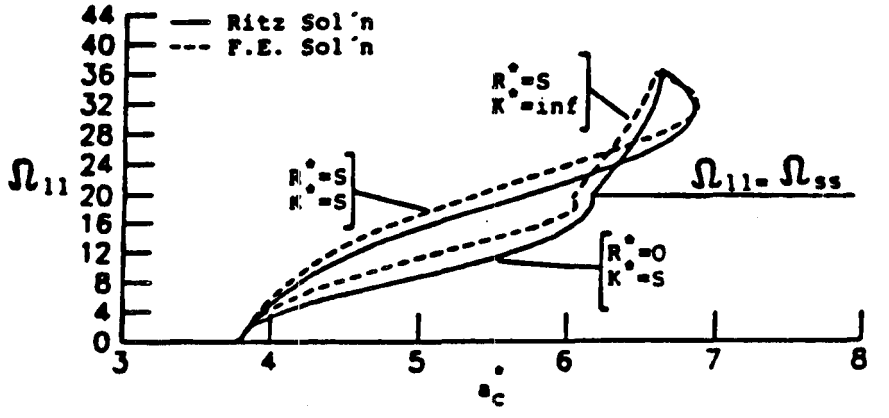

Figure (11). Variation of center acceleration with respect to fundamental frequency parameter, Ω_{11}, of a square plate with translational and rotational restraint parameters. Identical boundary conditions on all edges. Sinusoidal load at fundamental frequency, f_{11}.

Figures (12) and (13) show the variation of strain at a point near the center of the plate. Figure (12A) displays the variation as the plate boundaries move from the clamped

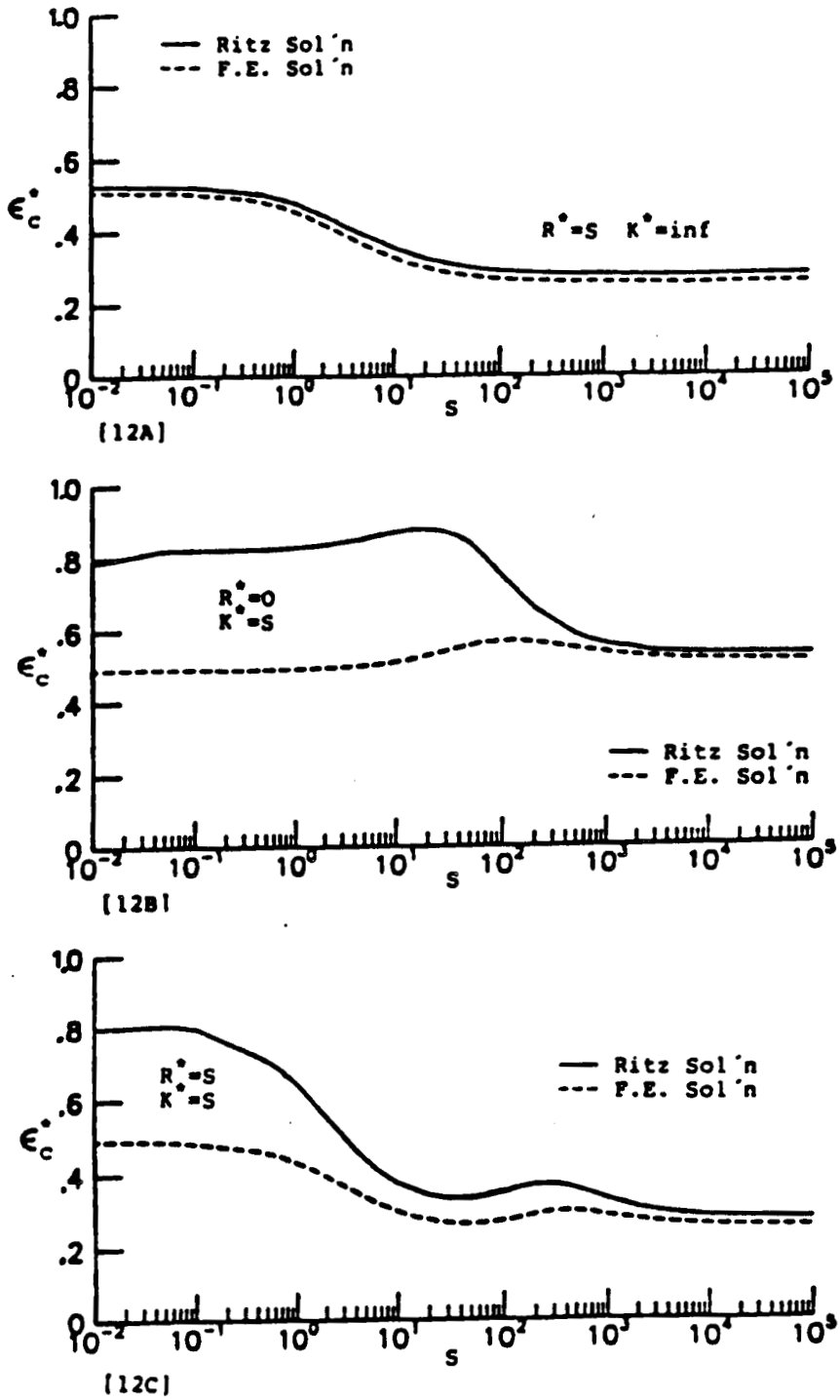

Figure (12). Variation of center strain with respect to restraint parameter, S, of a square plate with translational and rotational restraint parameters. Identical boundary conditions on all edges. Sinusoidal load at fundamental frequency, f_{11}.

to the simply-supported states. The agreement in that region is good. In figures (12B) and (12C) it is seen that as the plate edges are relaxed toward the free state, the agreement

between the two solutions deteriorates. As the elastic restraints are relaxed to values below 10^3, the NASTRAN solution gives decidedly lower results. There is , however, agreement in trend. That is, the magnitude of strain tends to rise and fall in similar fashion for both solutions. This agreement is more apparent in figure (13). The shapes of the closed curves are very similar in the prediction of high and low values of strain.

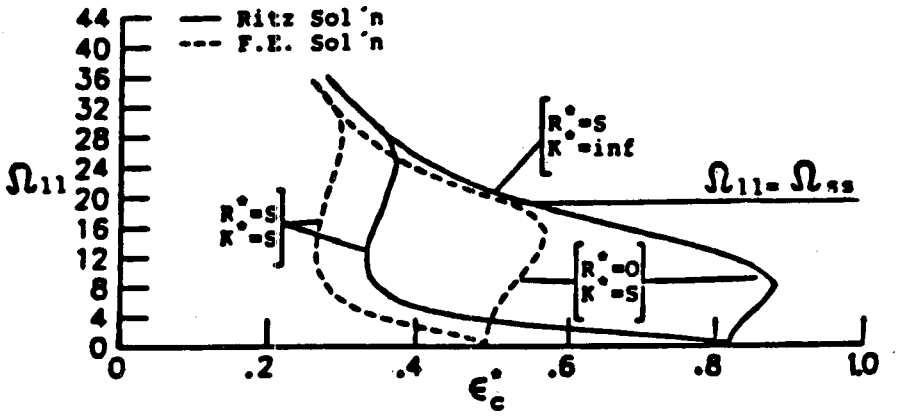

Figure (13). Variation of center strain with respect to fundamental frequency parameter, Ω_{11}, of a square plate with translational and rotational restraint parameters. Identical boundary conditions on all edges. Sinusoidal load at fundamental frequency, f_{11}.

The final comparison of response is taken from the results given in reference (5). In that work, the search for causes of a large bias error between experimentally measured and analytically predicted strain response led to the examination of the effect of both types of boundary springs on the response. For that study, only the finite element method was used to model a plate whose edges were elastically restrained in rotation and transverse translation since no other method was available at the time. The response was calculated for

various combinations of selected values of restraint while maintaining a constant fundamental frequency. At one end of the scale, the plate possesses infinite rotational boundary spring stiffness with a finite value of transverse boundary spring stiffness. At the other end of the scale, the reverse is true. Combinations of finite values for both types of boundary spring fill in table (12).

The NASTRAN finite element results as given in reference (5) have been non-dimensionalized and the elastic Ritz solution has been used for comparison. The fundamental frequency

Comparison of Displacement and Strain for Various Translational and Rotational Restraint Values
$K_1=K_2=K_3=K_4=K \quad R_1=R_2=R_3=R_4=R$
Square Plate

Sinusoidal Load @ f_{11}

$\Omega_{11} = 26.57 \pm 5\%$

Rb/D	Kb^3/D	w_c^*	ϵ_c^*	ϵ_{edge}^*	
6.349	inf	0.0237 0.0256	0.3778 0.3802	0.2250 0.2233	$ $$
7.619	3108.573	0.0240 0.0260	0.3807 0.3802	0.2522 0.2474	$ $$
9.269	1334.86	0.0247 0.0262	0.3869 0.3782	0.2834 0.2736	$ $$
9.524	1261.713	0.0248 0.0264	0.3871 0.3782	0.2873 0.2776	$ $$
12.698	731.426	0.0258 0.0266	0.3933 0.3721	0.3298 0.3158	$ $$
25.396	438.86	0.0269 0.0268	0.3916 0.3560	0.4034 0.3842	$ $$
38.095	384.0	0.0271 0.0266	0.3868 0.3460	0.4301 0.4103	$ $$
63.492	338.286	0.0274 0.0267	0.3817 0.3379	0.4527 0.4345	$ $$
inf	292.573	0.0274 0.0267	0.3685 0.3198	0.4846 0.4727	$ $$

$ Ritz solution herein
$$ Nastran F.E. Solution

Table (12)

prediction for given values of restraint varied by no more than 5%. The results of table (12) show good comparison for center displacement which seems to remain relatively constant. The near center strain given by NASTRAN tends to drop slightly while the elastic Ritz solution gives relatively constant values. The near edge strain from a point midway along one of the edges increases as the translational restraint relaxes and the rotational restraint is tightened. This comparison validates the conclusions of reference (5), since the introduction of transverse motion at the boundaries could not account for the bias error.

CHAPTER 6

Conclusions

Conclusions from Comparisons

Many authors have addressed the problem of free vibration of uniform rectangular plates. An informative survey of recent studies was given by Leissa (20). Most of the studies were restricted to plates possessing the classical free, clamped and simply-supported edge conditions and in some cases, the academic agreement on accepted theoretical frequencies is still open to debate.

Many methods have been derived and used in an effort to calculate more accurate frequencies with ease of computation. With the ability of the computer to perform complicated calculations at high speed, the ease of computation is not as important as it once was. In fact, one of the reasons early derivations of solution were simplified was to yield expressions that were easier to use in the absence of efficient computer methods. The work given by Carmichael (13) in 1959 is a case in point. The assumption of symmetric boundary conditions with equal rotational restraint on parallel edges gave a simple explicit expressions for difficult integrals in the application of the Rayleigh-Ritz method.

The Ritz method is one of the more popular approximations used in plate vibrations since it has proven to be a straight forward valid approach. The accuracy returned by this method depends in large part on the functions chosen to represent displacement. In general, the accuracy of results can not be estimated with certainty. The frequencies can only be said to be higher than the true values. By satisfying the shear and moment boundary conditions, when applicable, the rate of convergence is aided. For plates without exact solutions (ie. no parallel simply-supported edges), the convergence rate is further enhanced by the use of beam functions. The indications are that the "best" estimates of frequency result when beam functions are selected so as to satisfy the edge conditions exactly. This choice of functions renders good approximations of frequency when only the single term (diagonal terms) expressions are used. Even frequencies of higher modes can be estimated with suitable accuracy using the single term solution.

For example, Young (21) discussed the use of the Ritz method for plate vibrations and assumed beam functions to represent displacements. For the square cantilever plate which is a case of unsymmetric boundary conditions, he chose the free-free and free-clamped beam functions for the two coordinate directions, respectively. Frequency calculations were based on an 18 term series. For the first mode, Young gave the value of the dimensionless frequency parameter as 3.494. A single term approximation based on the same beam functions

gives the fundamental parameter as 3.515 for a percent difference of 0.6%. On the fourth mode, the 18 term solution yields a value of 27.46 and the single term approximation gives 28.78 for a 4.8% difference. Nassar (22) extended the single term approach to include plates with rotationally restrained edges. The boundaries were assumed to be unsymmetric in restraining value. Functions were chosen as a weighted sum of clamped and simply-supported beam functions. A single term solution was also generated assuming beam functions of an unsymmetric rotationally restrained beam. Both solutions gave fundamental frequency predictions that varied from published results by no more than 0.5%.

In this study, a single term solution is again applied. The plate was assumed to be elastically restrained in both rotation and transverse translation. The edge spring values were assumed unsymmetric. For the comparisons of characteristic frequency parameter, it was seen that good results were achieved for all cases when the edge translation was completely constrained (ie. K=inf). In these cases, the edge conditions are between the simply-supported and clamped states, inclusively. When compared to the solution given by Carmichael in table (1), both the new elastic Ritz and NASTRAN finite element solutions gave good results. If an exact value of infinity for translational edge stiffness were applied to the new elastic Ritz solution, it would become equivalent to Carmichael's approximation.

The further comparisons of frequency parameter for plates rigid in edge translation showed acceptable agreement to the published results. The elastic Ritz and finite element results were equally valid for cases of unequal rotational restraint. For these cases, presented in tables (2), (5), (8), (9) and (10), the predictions of this study never differed by more than 1%. The frequency parameter comparisons made to available data for higher modes were within 5%. This indicates that the new results were soundly derived from valid approaches.

When both types of spring were activated simultaneously at the plate boundaries so that transverse edge motion was introduced, discrepancies in frequency prediction were encountered. Referring to figures (6) and (7), it was shown that the elastic Ritz and NASTRAN solutions agreed with the results of Warburton and Edney (12) when either of the two spring types acted alone. However, when both translational and rotational boundary springs were active, the two solutions of this study gave significantly lower frequencies. For all subsequent comparisons to published results for cases when restrained transverse motion was allowed at the edges, lower frequencies were again predicted by the methods used herein. Assuming no numerical error was present, since double checks uncovered none, this indicates that the choice of displacement functions becomes increasingly important. By considering the boundary conditions along with the choice of functions used in reference (12), the following is noted. For cases where the boundary conditions are between simply-supported and clamped

(ie. top curve of figures (6) and (7)), Warburton and Edney utilized a weighted sum of simply-supported and clamped beam functions. As such, the zero displacement edge condition was satisfied exactly while the moment condition is approximated through the range of elastic values with good results. On the lowest curve of those figures, a weignted sum of free and simply-supported beam functions were used. These functions satisfy the zero moment boundary condition exactly and approximate the shear condition over the range of elastic values. Again, by satisfying at least one of the boundary conditions, good results were achieved. For the intermediate curve where both types of spring were simultaneously active, the functions used in reference (12) were a weighted sum of simply-supported, clamped, free and sliding beam functions and collectively satisfy neither the shear or moment edge conditions. Rayleigh's principle guarantees the frequency predictions will be high by the argument of upper bounded eigenvalues. The weighted approximation on both types of elastic edge condition gives inflated results to the point of unpracticle accuracy. Unfortunately, one of the purposes of the published article was to give quick and easy frequency predictions with suitable accuracy.

The additional comparisons given by tables (3), (4), (6) and (7) for cases when restrained transverse motion is allowed at the edges showed similar results. The solutions of this study gave lower predictions of frequency for all cases except those of table (6) where the finite element predictions

were inconsistent. The reason for the inflated results was discovered. Accidentally, the pair of parallel edges that varied from simply-supported to free states had been over constrained. For plates with unequal translational restraint on boundaries, transverse edge displacement is not equal on all edges. As a result, the boundary nodal displacements on the finite element model must have freedom of rotation about an axis perpendicular to the edge. This rotational freedom was inadvertently constrained for the computer runs of table (6). When this was corrected, the NASTRAN solution agreed with the elastic Ritz predictions. At a value of $K^{*}=10$ in the top row of the table, the finite element dimensionless frequency parameter was found to be 11.25 compared to 11.31 for the elastic Ritz solution. The SS-Fr-SS-Fr case has an exact value as given by Leissa. The finite element prediction with corrections returned a value of 9.659 as compared to 9.676 and 9.6314 for the elastic Ritz and exact values, respectively. Therefore, the earlier major discrepancy of frequency prediction between NASTRAN and the elastic Ritz solutions may be attributed to user error. The minor differences of results between these two solutions can be attributed to convergence considerations. It is noted that the frequency results from the two approximations used in this study are not consistently higher or lower in comparison. The single term Ritz solution is also guaranteed to be high by Rayleigh's principle while an insufficient number of elements on the finite element model will slow it's

convergence. For any given comparison, it is difficult to predict which of these factors will take precedence to give more agreeable estimates of frequency.

Extension of the single term Ritz solution to predict response is generally less reliable than frequency prediction. Warburton (23) demonstrated that the single term solution may give very good results for displacement based on the convergence rate. The stress/strain convergence is usually slower however, especially for plates exhibiting unsymmetric boundary conditions or aspect ratios not equal to one. In general, if convergence of natural frequencies is slow, the convergence for response calculations will be slower still. Therefore, for cases deviating far from the square plate with equal or symmetric edge conditions, a multiple mode calculation with more terms in the Ritz series is recommended.

The fundamental resonance displacement and acceleration results showed good comparison between the single mode Ritz and finite element solutions in figures (8), (9), (10) and (11). This indicates that the convergence for displacements in the Ritz solution is rapid enough for good estimates. Combining good natural frequency and displacement comparisons, the accelerations predicted by both methods are expected to agree. Figures (10) and (11) show general agreement.

The strain response values as seen in figures (12) and (13) are not as agreeable for the two methods in all cases. Several factors may account for this. The convergence of the single term Ritz solution is not guaranteed, as mentioned. As

well, the finite element solution results are only as good as the refinementof the plate modeling and the element displacement functions chosen. The deviation of NASTRAN strain values from the Ritz solution is seen to occur as restraining values fall below 10^3 on figures (12B) and (12C). In these regions, the displacements begin increasing at a greater rate (see figure (8)). The continuous distribution of strain over the plate domain can only be approximated by the finite element model and since stress is constant over a given element, the distribution from NASTRAN is piecewise linear. As a result, for larger displacements, this piecewise distribution will show greater deviation and is less reliable to approximate the continuous distribution. By increasing the number of elements or using mesh refinement in areas of interest, a better approximation should result.

Another factor to help explain the disagreement of strain between the two solutions concerns the modeling of edge bending. For any given element, the corners are subject to differing magnitudes of translational and rotational displacement. These differences result in shear and moment forces at the nodes. In the interior of the plate, continuity of displacement at the nodes joining elements cancels out these forces. That is, the forces on one element are equal and opposite to those of an adjoining element. At the edges, these effects are elastically restrained. As the stiffness of the elastic restraints are lessened, the forces at the edges of the model are neglected. As a result the edge elements are

subject to little or no bending. To properly account for this, it is suggested that numerically appropriate artificial support reactions and bending moments be applied at the boundaries to induce bending in the edge elements. This would increase the strain values returned by NASTRAN.

Table (12) gave displacement and strain values for various combinations of edge restraint. The agreement was good. The NASTRAN finite element results were taken from reference (5) and non-dimensionalized. In that article, the edge strains were shown to increase as the transverse boundary spring stiffness was decreased and the rotational edge flexibility was increased. Since the experimental strains were lower than those predicted by a factor of three, the introduction of restrained edge translation does not account for the bias error. The elastic Ritz results of this study have substantiated that claim.

For practical applications of the two approaches of this study, the following factors to be considered are summarized. The Ritz solution should be extended to a multiple mode solution with a greater number of terms. Although, the frequencies from a single term solution can be accurate, the convergence of solution to predict response will be enhanced. This will add to the complexity of solution since the off-diagonal terms in the frequency determinant and contributions to response of higher modes in the determination of amplitude coefficients will be included in the analysis. The use of subroutines available in math and science software libraries

to solve the eigenvalue problem and matrix simultaneous equations should ease the burden. Also, the finite element model should be adjusted with a greater number of elements or mesh refinement in the areas of stress calculations. An increased number of elements would allow for a better approximation of the mode shapes by the finite element model. The edges should also be modeled with proper reactions.

Comments on the Use of MACSYMA and NASTRAN

MACSYMA's evolution has been steady and methodical. The capabilities are continuously being expanded so that the program size is increasing rapidly. There are many problems in mathematics and in physical sciences to which MACSYMA has not been applied. For these reasons, it is impossible for one person to fully understand all of MACSYMA's capabilities. To the novice user, MACSYMA is somewhat of a "black box" that miraculously returns answers to complicated problems in mathematics.

In this study, MACSYMA was used to solve the simultaneous equations of boundary conditions in order to specify the functions that describe the normal modes of vibration of the elastically restrained beam. This is the most difficult part of the solution. It is assumed that this difficulty is the reason no published material on the use of these beam functions in plate vibrations was found. Although the derivation of the functions is difficult, it is not impossible to derive these functions by hand. In fact, they were derived by hand in order to assess that part of the contribution from

MACSYMA. The solution, when done by hand, comprised 14 pages. Care was taken to avoid mistakes (sign errors are a specialty) so that with simplifications and verification, the solution to get the beam functions took approximately 25 hours. When MACSYMA was applied, the most time was spent on problem setup. Once the input of the boundary equations was done and the general expressions for tne beam functions were substituted into those equations, MACSYMA returned the completed solution for coefficients and the transcendental equation to determine the argument, alph(m), in about five minutes. Indeed, the expressions given by MACSYMA before simplification were fairly compact and programmable.

MACSYMA was also used to perform all integration necessary to form the Rayleigh quotient and the work of the pressure load on the plate. The expressions from equations (22) through (26) for displacement and strain were derived completely on the computer. The entire analytical solution was done using MACSYMA.

Once expressions were simplified to the desired degree, the Fortran code was generated. Fortran routines were written and debugged as the solution derivation progressed. When the solution for the coefficients and argument of the beam functions was complete, the Newton-Raphson subroutine was written and verified. The necessary Fortran subroutine for calculation of the integral expressions and the formation of the Rayleigh quotient was written once progress of analytic derivation permitted. Finally the expressions for displacement and strain

were derived and the response routine was programmed. The solution was complete. The derivation and programming of the entire Ritz algorithm was done on the computer. The major role of this user was to keep track of the necessary steps and to debug the Fortran program.

One of the features of MACSYMA is the share directory. The share directory is a library of special math routines that were written by MACSYMA users and incorporated into the software for general use. As more physicists and engineers become aware of symbolic manipulation systems, these share directories will begin to branch out. General solution algorithms to problems in the physical sciences will become available. For example, the Ritz procedure for plate vibrations might be incorporated into the system. The interactive user will input the functions and specify the boundary conditions. The software will grind out the necessary expressions and return a complete solution for natural frequencies. At the touch of a button, the Fortran code is given and numerical evaluations begin. Of course this is an over simplification but it is not an unrealistic concept.

NASTRAN, like MACSYMA, is a large software package that no one user can completely grasp. It is therefore also a "black box" system. The user must be sure to follow the rules and format the input correctly in order to properly model the problem. The results of table (6) were not corrected in this manuscript since they serve as an example. In the long formatted input listing, a single digit caused erroneous results.

One of the problems encountered in the course of this study was the length of time required and amount of storage needed by NASTRAN. Typical runs of NASTRAN, which required the loading of the 15 modules that comprise the extensive package, used about five minutes of CPU time on the Cyber 175 system. In one instance, the number of degrees of freedom on the plate were increased nine-fold. That is, the number of elements was increased to check frequency convergence. The required CPU time was likewise increased nine-fold. Since the NASTRAN runs were made on a time share computer system, generating results was often frustrating and always time consuming. Runs were required to determine natural frequencies and again to apply an harmonic load at the fundamental frequency. As a result, NASTRAN did not lend itself conveniently to the parametric and response analyses of this study.

An advantage of NASTRAN is that it can analyze complex problems. The finite element method provides a means to examine problems where no analytical method is available. The capabilities of NASTRAN are extensive but they have a limit. Finite element formulations to problems that NASTRAN can not presently handle are being derived by researchers everyday. It is only a matter of time that these solutions will be incorporated into software packages such as NASTRAN.

A small fraction of the capabilities of both MACSYMA and NASTRAN were required for the analysis of this study. Therefore, this user must be considered a novice on both systems. The work did serve as a good introduction to the

available software. This introduction instilled an appreciation and respect for the capabilities of MACSYMA and NASTRAN that allows the following conclusions.

Any engineer that is involved in complicated derivations of solution should become aware of symbolic manipulation systems and consider their use. The time saving alone is a valuable asset. These systems also eliminate the chances of mistake that accompany long algebraic and calculus related manipulations. From the point of view of this user, computer aided mathematics is tremendously powerful tool for the engineer.

Finite element software has come of age. The capabilities of the available packages are always increasing. Even for problems where analytical solutions exist and are used, a finite element solution is a valid approach to check results or compare with experimental data.

BIBLIOGRAPHY

Works Cited

1. McGowan, P. R., "Stuctural Design for Acoustic Fatigue," ASD-TDR-63-820, Air Force Flight Dynamics Laboratory, Wright-Patterson AFB, Ohio, October 1963.

2. Thompson, A. G. and Lambert, R. F., "Acoustic Fatigue Design Data," Part II, AGARD-AG-162, Advisory Group for Aerospace Research and Development, North Atlantic Treaty Organization, November 1972.

3. Jacobson, M. J., "Sonic Fatigue Design Data for Bonded Aluminum Aircraft Structures," AFFDL-TR-77-45, Air Force Flight Dynamics Laboratory, Wright-Patterson AFB, Ohio, June 1977.

4. Roussos, L. A., Heitman, K. E. and Rucker, C. E., "Predicted and Measured Strain Response of Rectangular Panels due to Acoustic Loading," Presented at 10th AIAA Aeroacoustics Conference, Seattle, WA., July 9-11, 1986, AIAA paper no. 86-1931.

5. Roussos, L. A. and Brewer, T. K., "Effect of Boundary Conditions on Dynamic Strain Response of Rectangular Panels," Presented at AIAA Dynamics Specialists Conference, Monterey, CA., April 9-10, 1987, AIAA paper no. 87-0935.

6. Filipich, C. P., Reyes, J. A. and Rossi, R. E., "Free Vibrations of Rectangular Plates Elastically Restrained Against Rotation and Translation Simultaneously at the Four Edges," Journal of Sound and Vibration, Vol. 56, pp. 299-302, 1978.

7. Mukhopadhyay, M., "Free Vibrations of Rectangular Plates With Edges Having Different Degrees of Rotational Restraint," Journal of Sound and Vibration, Vol. 67, pp. 459-468, 1979.

8. Laura, P. A. A. and Grossi, R. O., "Transverse Vibrations of Rectangular Plates With Edges Elastically Restrained Against Translation and Rotation," Journal of Sound and Vibration, Vol. 75, pp. 101-107, 1981.

9. Laura, P. A. A., "Comments on ´ Vibrations of Rectangular Plates With Elastically Restained Edges´," Journal of Sound and Vibration, Vol. 101, pp. 589-590, 1985.

10. Warburton, G. B. and Edney, S. L., "Authors Reply to Comments on ´ Vibrations of Rectangular Plates With Elastically Restrained Edges´," Journal of Sound and Vibration, Vol. 101, pp. 590-591, 1985.

11. Leissa, A. W., "Free Vibration of Rectangular Plates," Journal of Sound and Vibration, Vol. 31, pp. 257-293, 1973.

12. Warburton, G. B. and Edney, S. L., "Vibrations of Rectangular Plates With Elastically Restrained Edges," Journal of Sound and Vibration, Vol. 95, pp. 537-552, 1984.

13. Carmichael, T. E., "The Vibration of a Rectangular Plate With Edges Elastically Restrained Against Rotation," Quarterly Journal of Mechanics and Applied Mathematics, Vol. 12, pp. 29-42, 1959.

14. Soedel, W., Vibrations of Plates and Shells , New York: Marcel Dekker, Inc., 1981, pp. 163.

15. Deloach, S., Instructor, MACSYMA Seminar, Given at NASA at Langley, Hampton, VA., Manuscript Handout, July, 1987

16. Pavelle, R, "MACSYMA: Capabilities and Applications to Problems in Engineering and the Sciences," Symbolics, Inc., 1985.

17. Field, E. I., Herting, D. N. and Morgan, M.J., NASTRAN User´s Guide (level 17.5), NASA CR 3146, June 1979.

18. McCormick, C. W. (editor), The NASTRAN User´s Manual, NASA SP-222(06), 1981.

19. MacNeal, R. H. (editor), The NASTRAN Theoretical Manual, NASA SP-221(06), 1981.

20. Leissa, A. W., "Recent Studies in Plate Vibrations: 1981-1985 Part I. Classical Theory," Shock and Vibration Digest, Vol. 19, pp. 11-18, 1987.

21. Young, D., "Vibration of Rectangular Plates by the Ritz Method," Journal of Applied Mechanics, Vol. 17, pp. 448-453, 1950.

22. Nassar, E. M., "Rapid Calculation of Resonance Frequency for Rotationally Restrained Rectangular Plates," AIAA Journal, Vol. 17, pp. 6-11, 1979.

23. Warburton, G. B., "Response Using the Rayleigh-Ritz Method," Earthquake Engineering and Structural Dynamics, Vol. 7, pp. 327-334, 1979.

Additional References

24. VAX UNIX MACSYMA Reference Manual, Version 11, Symbolics, Inc., 1985.

25. Craig, R. R., Structural Dynamics, New York: John Wiley & Sons, Inc., 1981.

26. Meirovitch, L., Computational Methods in Structural Dynamics, Alphen aan den Rijn, The Netherlands: Sijtoff & Noordhoff International Publishers B.V., 1980.

27. Warburton, G. W., "The Vibration of Rectangular Plates," Proceedings of the Institution of Mechanical Engineers, Vol. 168, pp. 371-381, 1954.

28. Laura, P. A. A., Luisoni, L. E. and Filipich, C., "A Note on the Determination of the Fundamental Frequency of Thin, Rectangular Plates with Edges Possessing Different Rotational Flexibility Coeficients," Journal of Sound and Vibration, Vol. 55, pp.327-333, 1977.

29. Lomas, N. S. and Hayek, S. I., "Vibration and Acoustic Radiation of Elastically Supported Rectangular Plates," Journal of Sound and Vibration, Vol. 52, pp. 1-25, 1977.

30. Ng, S. F. and Sharma, A., "Vibration of Thin Plates Using the Ritz Method," Aeronautics and Space Journal, Vol. 25 pp. 372-381, 1979.

31. Bhat, R. B., "Natural Frequencies of Rectangular Plates Using Characteristic Orthogonal Polynomials in the Rayleigh-Ritz Method," Journal of Sound and Vibration, Vol. 102, pp. 493-499, 1985.

APPENDIX A

Notation

It is noted here that MACSYMA does not recognize Greek nomenclature. Therefore, english abbreviations were used for those characters in all MACSYMA displays contained in this manuscript. Also, MACSYMA does not allow the use of upper and lower case characters simultaneously so that all MACSYMA displays are in lower case. For these reasons, the notation list below is expanded to include the MACSYMA notation used. The MACSYMA notations are enclosed in brackets '[]'.

x,y,z	Cooridinate directions.
a,b	Length (x direction) and width (y direction) of the plate, respectively.
h	Thickness (z direction) of the plate.
t	Time.
ω, f [nf_{mn}]	Radian and cyclic frequencies, respectively.
ρ, [rho]	Density (mass/unit volume).
c, ζ	Damping coeficient and % critical damping coeficient, respectively.
μ, [pr]	Poisson's ratio.
D, [d]	Flexural stiffness constant, $D=Eh^3/12(1-\mu^2)$, where E=Young's Modulus.
w(x,y,t)	Transverse displacement (z direction) where W(x,y) is seperated spatial variation.

p(x,y,t)	Normally incident pressure on plate surface where P(x,y) = P is uniform spatial variation over the surface.
V,T	Potential or strain energy and kinetic energy of the plate, respectively. V is associated with elastic energy in the plate and boundary springs.
Q	Work done on the plate by pressure, p(x,y,t).
$X_m(x), Y_n(y)$ [x(m), xm(x)] [y(n), yn(y)]	Beam functions in respective x and y directions chosen for transverse displacement variation, W(x,y).
A_{mn} [a(m,n)]	
B_m, C_m, D_m [b(m),c(m),d(m)]	Amplitude coeficients found in beam
E_n, F_n, G_n [e(n),f(n),g(n)]	functions representing W(x,y).
α_m,[alph(m)]	Characteristic values found in the arguments
β_n,[bet(n)]	of beam functions.
Ri,Ki [ri,ki]	Rotational and transverse translational restraint values, respectively.
r,i,m, n,p,q	Indices, (positive integers).
σ, ϵ	Stress and strain, respectively.
[cc,ss,chch shsh,cs,cch csh,sch,ssh chsh]	Integrals defined in Appendix C.
[xhm,xjm,xkm xlm,xosq,xasq xposq,xpasq xqm]	Integrals of beam functions defined in Appendix C.
[%e, %pi]	Euler constant, e=2.17182818 and π=3.14159265, respectively. Recognized by MACSYMA as given.
∇^4	Biharmonic differential operator defined as, $\frac{\partial^4}{\partial x^4} + 2\frac{\partial^4}{\partial x^2 y^2} + \frac{\partial^4}{\partial y^4}$

APPENDIX B

Derivation of Beam Functions

The equations defining the elastic boundary conditions that the assumed displacement function, W(x,y) must satisfy were given in equations (6′, 7′). These equations may be seperated so that $X_m(x)$ must satisfy equations (6A′, 6B′ 7A′, 7B′) and $Y_n(y)$ must satisfy equations (6C′, 6D′, 7C′, 7D′). Once the coefficients, (B, C, D) and argument, alph(m), of X_m are obtained, the corresponding coefficients, (E, F, G) and argument, bet(n), of Y_n can be determined by the substitution described in chapter 2.

Rewriting the boundary condition equations for X_m and utilizing MACSYMA we get,

$$\left(\frac{d}{dx}\,(xm(o))\right) r1 = d\left(\frac{d^2}{dx^2}\,(xm(o))\right) \tag{B1}$$

$$\left(\frac{d}{dx}\,(xm(a))\right) r2 = -\left(\frac{d^2}{dx^2}\,(xm(a))\right) d \tag{B2}$$

$$k1\ xm(o) = -d\left(\frac{d^3}{dx^3}\,(xm(o))\right) \tag{B3}$$

$$xm(a)\ k2 = \left(\frac{d^3}{dx^3}(xm(a))\right) d \qquad \text{(B4)}$$

Substituting the expression for X_m given in equation (10), differentiating and evaluating the appropriate equations at x=o and x=a, equations (B1, B2, B3, B4) become,

$$\left(\frac{alph(m)\ c(m)}{a} + \frac{alph(m)\ b(m)}{a}\right) r1 = d\left(\frac{alph^2(m)\ d(m)}{a^2} - \frac{alph^2(m)}{a^2}\right) \qquad \text{(B5)}$$

$$\left(\frac{alph(m)\ d(m)\ \sinh(alph(m))}{a} - \frac{alph(m)\ \sin(alph(m))}{a} + \frac{alph(m)\ b(m)\ \cosh(alph(m))}{a} + \frac{alph(m)\ c(m)\ \cos(alph(m))}{a}\right) r2 =$$

$$- d\left(\frac{alph^2(m)\ b(m)\ \sinh(alph(m))}{a^2} - \frac{alph^2(m)\ c(m)\ \sin(alph(m))}{a^2} + \frac{alph^2(m)\ d(m)\ \cosh(alph(m))}{a^2} - \frac{alph^2(m)\ \cos(alph(m))}{a^2}\right) \qquad \text{(B6)}$$

$$k1\ (d(m) + 1) = - d\left(\frac{alph^3(m)\ b(m)}{a^3} - \frac{alph^3(m)\ c(m)}{a^3}\right) \qquad \text{(B7)}$$

$$k2\,(b(m)\,\sinh(alph(m)) + c(m)\,\sin(alph(m))$$

$$+\ d(m)\,\cosh(alph(m)) + \cos(alph(m))) =$$

$$d\left(\frac{alph^3(m)\,d(m)\,\sinh(alph(m))}{a^3} + \frac{alph^3(m)\,\sin(alph(m))}{a^3}\right.$$

$$\left. + \frac{alph^3(m)\,b(m)\,\cosh(alph(m))}{a^3} - \frac{alph^3(m)\,c(m)\,\cos(alph(m))}{a^3}\right)$$

(B8)

Using equations (B5, B7, B8) and solving simultaneously for B_m, C_m and D_m, MACSYMA gives,

$$b(m) = (-\,(a^4\,d\,k1\,alph^3(m)$$

$$(\sinh(alph(m)) - \sin(alph(m)))$$

$$+\ a^7\,k1\,(k2\,\cos(alph(m)) - k2\,\cosh(alph(m)))\,r1$$

$$-\ d^3\,alph^7(m)\,(\sinh(alph(m)) + \sin(alph(m)))$$

$$+\ 2\,a^6\,d\,k1\,k2\,alph(m)\,\sin(alph(m))$$

$$-\ a^3\,d^2\,alph^4(m)\,(-\,k2\,\cosh(alph(m)) - k2\,\cos(alph(m))$$

$$-\ 2\,k1\,\cos(alph(m))))/denominator$$

(B9)

$$c(m) = ((a^4 d\, kl\, alph^3(m)$$

$$(\sinh(alph(m)) - \sin(alph(m)))$$

$$+ a^7 kl\, (k2 \cos(alph(m)) - k2 \cosh(alph(m)))\, rl$$

$$- 2\, a^6 d\, kl\, k2\, alph(m) \sinh(alph(m))$$

$$+ d^3 alph^7(m)\, (-\sinh(alph(m)) - \sin(alph(m)))$$

$$+ a^3 d^2 alph^4(m)\, (k2 \cosh(alph(m)) + 2\, kl \cosh(alph(m))$$

$$+ k2 \cos(alph(m))))/denominator \qquad (B10)$$

$$d(m) = (-(a^7 kl\, (k2 \sinh(alph(m)) - k2 \sin(alph(m)))$$

$$+ 2\, a\, d^2 alph^6(m) \sin(alph(m))$$

$$+ a^4 d\, alph^3(m)\, (kl\, (-\cosh(alph(m)) - \cos(alph(m)))$$

$$- 2\, k2 \cos(alph(m)))\, rl - a^3 d^2 alph^4(m)$$

$$(k2 \sinh(alph(m)) + k2 \sin(alph(m)))$$

$$- d^3 alph^7(m)\, (\cos(alph(m)) - \cosh(alph(m))))/denominator$$

(B11)

where,

$$denominator = (a^7 kl\, (k2 \sinh(alph(m))$$

$$- k2 \sin(alph(m))) + 2\, a\, d^2 alph^6(m) \sinh(alph(m))$$

$$+ a^4 d\, alph^3(m)\, (kl\, (-\cosh(alph(m)) - \cos(alph(m)))$$

$$- 2\,k2\,\cosh(\mathrm{alph}(m)))))\,r1 + a^3\,d^2\,\mathrm{alph}^4(m)$$

$$(-\,k2\,\sinh(\mathrm{alph}(m)) - k2\,\sin(\mathrm{alph}(m)))$$

$$+\,d^3\,\mathrm{alph}^7(m)\,(\cosh(\mathrm{alph}(m)) - \cos(\mathrm{alph}(m))) \qquad \text{(B12)}$$

Equation (B6) can be rewritten as,

$$\left(\frac{\mathrm{alph}(m)\,d(m)\,\sinh(\mathrm{alph}(m))}{a} - \frac{\mathrm{alph}(m)\,\sin(\mathrm{alph}(m))}{a}\right.$$

$$\left. + \frac{\mathrm{alph}(m)\,b(m)\,\cosh(\mathrm{alph}(m))}{a} + \frac{\mathrm{alph}(m)\,c(m)\,\cos(\mathrm{alph}(m))}{a}\right)$$

$$r2 + d\left(\frac{\mathrm{alph}^2(m)\,b(m)\,\sinh(\mathrm{alph}(m))}{a^2}\right.$$

$$\left. - \frac{\mathrm{alph}^2(m)\,c(m)\,\sin(\mathrm{alph}(m))}{a^2} + \frac{\mathrm{alph}^2(m)\,d(m)\,\cosh(\mathrm{alph}(m))}{a^2}\right.$$

$$\left. - \frac{\mathrm{alph}^2(m)\,\cos(\mathrm{alph}(m))}{a^2}\right) = 0$$

(B13)

and substitution of equations (B9, B10, B11, B12) into (B13) results in the transcendental equation that is used to solve for alph(m).

The solution of equation (B13) was done numerically by Newton-Raphson method which necessitates the determination of the derivative of the left-hand side of equation (B13) with respect to alph(m). MACSYMA was used for this calculation, however the expression is quite long and not included here.

APPENDIX C

Calculation of Beam Integrals

The integrals necessary in the calculation of the Rayleigh quotient for natural frequencies and subsequently the work done on the plate for forced response were given in equations (2, 3, 16, 17 and 19). These integrals are evaluated by inserting the expressions assumed for the mode displacement functions (equations (10 and 11). Since these functions are separable and similar in x and y, the integrals may be evaluated independently for x and similar expressions for y are obtained by the substitution described in chapter 2.

Inserting the expression for X_m (x) into the integrands of the appropriate integrals and expanding these integrand expressions, the following integrals are needed.

$$cc = \int_0^a \cos\left(\frac{2\,alph(m)\,x}{a}\right) dx \qquad (C1)$$

$$ss = \int_0^a \sin\left(\frac{2\,alph(m)\,x}{a}\right) dx \qquad (C2)$$

$$chch = \int_0^a \cosh\left(\frac{2\,alph(m)\,x}{a}\right) dx \qquad (C3)$$

$$shsn = \int_0^a \sinh\left(\frac{2\,alph(m)\,x}{a}\right) dx \qquad (C4)$$

$$cs = \int_0^a \cos\left(\frac{alph(m)\,x}{a}\right) \sin\left(\frac{alph(m)\,x}{a}\right) dx \qquad (C5)$$

$$ccn = \int_0^a \cos\left(\frac{alph(m)\,x}{a}\right) \cosh\left(\frac{alph(m)\,x}{a}\right) dx \qquad (C6)$$

$$csh = \int_0^a \cos\left(\frac{alph(m)\,x}{a}\right) \sinh\left(\frac{alph(m)\,x}{a}\right) dx \qquad (C7)$$

$$sch = \int_0^a \cosh\left(\frac{alph(m)\,x}{a}\right) \sin\left(\frac{alph(m)\,x}{a}\right) dx \qquad (C8)$$

$$ssh = \int_0^a \sin\left(\frac{alph(m)\,x}{a}\right) \sinh\left(\frac{alph(m)\,x}{a}\right) dx \qquad (C9)$$

$$chsh = \int_0^a \cosh\left(\frac{alph(m)\,x}{a}\right) \sinh\left(\frac{alph(m)\,x}{a}\right) dx \qquad (C10)$$

In general, MACSYMA converts the hyperbolic sine and hyperbolic cosine (sinh and cosh) into exponential form as an aid to integration by the familiar identities,

$$\cosh(u) = \frac{\%e^{u} + \%e^{-u}}{2}, \quad \sinh(u) = \frac{\%e^{u} - \%e^{-u}}{2} \qquad (C11, C12)$$

After integration, MACSYMA does not recombine the exponential terms and gives,

$$cc = \frac{a \sin(2\,alph(m)) + 2\,a\,alph(m)}{4\,alph(m)} \qquad (C13)$$

$$ss = -\frac{a \sin(2\,alph(m)) - 2\,a\,alph(m)}{4\,alph(m)} \qquad (C14)$$

$$chch = \frac{\%e^{-2\,alph(m)}\,(a\,\%e^{4\,alph(m)} + 4\,a\,alph(m)\,\%e^{2\,alph(m)} - a)}{8\,alph(m)} \qquad (C15)$$

$$shsh = \frac{\%e^{-2\,alph(m)}\left(a\,\%e^{4\,alph(m)} - 4\,a\,alph(m)\,\%e^{2\,alph(m)} - a\right)}{8\,alph(m)} \qquad (C16)$$

$$cs = \frac{a\,\sin^2(alph(m))}{2\,alph(m)} \qquad (C17)$$

$$cch = \frac{a\,\%e^{alph(m)}\sin(alph(m))}{4\,alph(m)} + \frac{a\,\%e^{-alph(m)}\sin(alph(m))}{4\,alph(m)} + \frac{a\,\%e^{alph(m)}\cos(alph(m))}{4\,alph(m)} - \frac{a\,\%e^{-alph(m)}\cos(alph(m))}{4\,alph(m)} \qquad (C18)$$

$$csh = \frac{a\,\%e^{alph(m)}\sin(alph(m))}{4\,alph(m)} - \frac{a\,\%e^{-alph(m)}\sin(alpn(m))}{4\,alph(m)} + \frac{a\,\%e^{alph(m)}\cos(alph(m))}{4\,alph(m)} + \frac{a\,\%e^{-alph(m)}\cos(alph(m))}{4\,alph(m)} - \frac{a}{2\,alph(m)} \qquad (C19)$$

$$sch = \frac{a\,\%e^{alph(m)}\sin(alph(m))}{4\,alph(m)} - \frac{a\,\%e^{-alph(m)}\sin(alph(m))}{4\,alph(m)} - \frac{a\,\%e^{alph(m)}\cos(alph(m))}{4\,alph(m)} - \frac{a\,\%e^{-alph(m)}\cos(alph(m))}{4\,alph(m)} + \frac{a'}{2\,alph(m)} \qquad (C20)$$

$$ssh = \frac{a\,\%e^{alph(m)}\,sin(alph(m))}{4\,alph(m)} + \frac{a\,\%e^{-alph(m)}\,sin(alph(m))}{4\,alph(m)} - \frac{a\,\%e^{alph(m)}\,cos(alph(m))}{4\,alph(m)} + \frac{a\,\%e^{-alph(m)}\,cos(alph(m))}{4\,alph(m)} \qquad (C21)$$

$$chsh = \frac{a\,cosh^{2}(alph(m))}{2\,alph(m)} - \frac{a}{2\,alph(m)} \qquad (C22)$$

By recognizing the hyperbolic terms and simplifying according to the identities of equations (C11 and C12) the exponential expressions may be reduced to,

$$chch = (a/4alph(m))\,(sinh(2alph(m))+2alph(m)) \qquad (C23)$$

$$shsh = (a/4alph(m))\,(sinh(2alph(m))-2alph(m)) \qquad (C24)$$

$$cch = (a/2alph(m))\,(sin(alph(m))cosh(alph(m)) + cos(alph(m))sinh(alph(m))) \qquad (C25)$$

$$csh = (a/2alph(m))\,(sin(alph(m))sinh(alph(m)) + cos(alph(m))cosh(alph(m))-1) \qquad (C26)$$

$$sch = (a/2alph(m))\,(sin(alph(m))sinh(alph(m)) - cos(alph(m))cosh(alph(m))+1) \qquad (C27)$$

$$ssh = (a/2alph(m))\,(sin(alph(m))cosh(alph(m)) - cos(alph(m))sinh(alph(m))) \qquad (C28)$$

The integrals that result from the insertion of $X_m(x)$ are then defined as,

$$xhm = \int_0^a xm^2(x)\,dx \tag{C29}$$

$$xjm = \int_0^a \left(\frac{d}{dx}(xm(x))\right)^2 dx \tag{C30}$$

$$xkm = \int_0^a \left(\frac{d^2}{dx^2}(xm(x))\right)^2 dx \tag{C31}$$

$$xlm = \int_0^a xm(x)\left(\frac{d^2}{dx^2}(xm(x))\right) dx \tag{C32}$$

and can be shown to be given by,

$$\begin{aligned} xhm = {} & b(m)\,b(m)\,shsh + 2\,b(m)\,c(m)\,ssh + 2\,b(m)\,d(m)\,shch \\ & + 2\,b(m)\,csh + c(m)\,c(m)\,ss + 2\,c(m)\,d(m)\,sch \\ & + 2\,c(m)\,cs + d(m)\,d(m)\,chch + 2\,d(m)\,cch + cc \end{aligned} \tag{C33}$$

$$\begin{aligned} xjm = {} & (alph(m)/a)^2\,(d(m)\,d(m)\,shsh - 2\,d(m)\,ssh \\ & + 2\,b(m)\,d(m)\,shch + 2\,c(m)\,d(m)\,csh + ss \\ & - 2\,b(m)\,sch - 2\,c(m)\,cs + b(m)\,b(m)\,chch \\ & + 2\,b(m)\,c(m)\,cch + c(m)\,c(m)\,cc) \end{aligned} \tag{C34}$$

$$xkm = (alph(m)/a)^4 \, (b(m)\, b(m)\, shsh - 2\, b(m)\, c(m)\, ssh + 2\, b(m)\, d(m)\, shch - 2\, b(m)\, csh + c(m)\, c(m)\, ss - 2\, c(m)\, d(m)\, sch + 2\, c(m)\, cs + d(m)\, d(m)\, chch - 2\, d(m)\, cch + cc) \tag{C35}$$

$$xlm = (alph(m)/a)^2 \, (b(m)\, b(m)\, shsh + 2\, b(m)\, d(m)\, shch - c(m)\, c(m)\, ss - 2\, c(m)\, cs + d(m)\, d(m)\, chch - cc) \tag{C36}$$

The final necessary expressions for the determination of natural frequencies arise from the elastic restraint energy terms of equations (16 and 17). Letting $[X_m(o)]^2$=xosq, $[X_m(a)]^2$=xasq, $[X'_m(o)]^2$=xposq and $[X'_m(a)]^2$=xpasq where ' indicates the derivative with respect to x, then,

$$xosq = (d(m) + 1)^2 \tag{C37}$$

$$\begin{aligned} xasq = {} & b^2(m)\, \sinh^2(alph(m)) \\ & + 2\, b(m)\, c(m)\, \sin(alph(m))\, \sinh(alph(m)) \\ & + 2\, b(m)\, d(m)\, \cosh(alph(m))\, \sinh(alph(m)) \\ & + 2\, b(m)\, \cos(alph(m))\, \sinh(alph(m)) + c^2(m)\, \sin^2(alph(m)) \\ & + 2\, c(m)\, d(m)\, \cosh(alph(m))\, \sin(alph(m)) \\ & + 2\, c(m)\, \cos(alph(m))\, \sin(alph(m)) + d^2(m)\, \cosh^2(alph(m)) \\ & + 2\, d(m)\, \cos(alph(m))\, \cosh(alph(m)) + \cos^2(alph(m)) \end{aligned} \tag{C38}$$

$$xposq = \frac{alph^2(m)\, (c(m) + b(m))^2}{a^2} \tag{C39}$$

$$xpasq = alph^2(m)\,(d^2(m)\,sinh^2(alph(m))$$
$$- 2\,d(m)\,sin(alph(m))\,sinh(alph(m))$$
$$+ 2\,b(m)\,d(m)\,cosh(alph(m))\,sinh(alph(m))$$
$$+ 2\,c(m)\,d(m)\,cos(alph(m))\,sinh(alph(m)) + sin^2(alph(m))$$
$$- 2\,b(m)\,cosh(alph(m))\,sin(alph(m))$$
$$- 2\,c(m)\,cos(alph(m))\,sin(alph(m)) + b^2(m)\,cosh^2(alph(m))$$
$$+ 2\,b(m)\,c(m)\,cos(alph(m))\,cosh(alph(m))$$
$$+ c^2(m)\,cos^2(alph(m)))/a^2 \qquad (C40)$$

Again, similar expressions may be obtained for integrals of $Y_n(y)$ and it's derivatives by the substitution described on page 18 (chapter 2).

The Rayleigh quotient can be formed as,

$$\omega^2 = [D\,(xkm\,yhn + xhm\,ykn + 2\,\mu\,xlm\,yln + 2\,(1-\mu)\,xjm\,yjn)$$
$$+ R_1\,xposq\,yhn + R_2\,xpasq\,yhn + R_3\,yposq\,xhm + R_4\,ypbsq\,xhm$$
$$+ K_1\,xosq\,yhn + K_2\,xasq\,yhn + K_3\,yosq\,xhm + K_4\,ybsq\,xhm] \Big/ [\rho\,h\,xhm\,yhn] \qquad (C41)$$

Finally, the integration defined by equation (19) for the work of the uniform pressure on the plate is needed in order to calculate the amplitude coeficients, A_{mn}. This integral can be written for $X_m(x)$ as,

$$xqm = \left[\int_0^a xm(x)\,dx\right] \qquad (C42)$$

and is evaluated as,

```
xqm = a (d(m) sinh(alph(m)) + sin(alph(m))
+ b(m) cosh(alph(m)) - c(m) cos(alph(m)) + c(m) - b(m))
/alph(m)
```

(C43)

APPENDIX D

Solution for Coeficients of Rayleigh-Ritz Series

The equation used to determine the coeficients (A_{mn}) of the Rayleigh-Ritz series was given in chapter 2 (equation (22)). Substitution of the assumed displacement functions (equations (10 and 11) and the integral expressions from Appendix C, equation (22) can be written as,

$$\frac{\partial}{\partial A_{mn}}\left(\rho \frac{h}{2} \omega^2 A_{mn}^2 \, xhm \, yhn\right)\left(1 - \frac{\omega_{mn}^2}{\omega^2}\right) = \frac{\partial}{\partial A_{mn}}\left(-P \, A_{mn} \, xqm \, yqn\right) \tag{D1}$$

or,

$$\left(A_{mn} \, \rho \, h \, \omega^2 \, xhm \, yhn\right)\left(1 - \frac{\omega_{mn}^2}{\omega^2}\right) = -P \, xqm \, yqn \tag{D2}$$

Solving for A_{mn},

$$A_{mn} = \frac{-P \, xqm \, yqn}{\rho \, h \, \omega^2 \, xhm \, yhn \left(1 - \frac{\omega_{mn}^2}{\omega^2}\right)}$$

$$= \frac{-P \, xqm \, yqn}{\rho \, h \, xhm \, yhn \left(\omega_{mn}^2 - \omega^2\right)} \tag{D3}$$

Equation (D3) is for the undamped case. Damping can be incorporated into the solution in the form of percent critical damping by adding $i2\zeta\omega_{mn}\omega$ to $(\omega_{mn}^2 - \omega^2)$ in the denominator.